

# Poly(Sarcosine)-Based Nano-Objects with Multi-Protease Resistance by Aqueous Photoinitiated Polymerization-Induced Self-Assembly (Photo-PISA)

Varlas, Spyridon; Georgiou, Panagiotis G; Bilalis, Panayiotis; Jones, Joseph R; Hadjichristidis, Nikos; O'Reilly, Rachel K

DOI:

[10.1021/acs.biomac.8b01326](https://doi.org/10.1021/acs.biomac.8b01326)

License:

Other (please specify with Rights Statement)

*Document Version*

Peer reviewed version

*Citation for published version (Harvard):*

Varlas, S, Georgiou, PG, Bilalis, P, Jones, JR, Hadjichristidis, N & O'Reilly, RK 2018, 'Poly(Sarcosine)-Based Nano-Objects with Multi-Protease Resistance by Aqueous Photoinitiated Polymerization-Induced Self-Assembly (Photo-PISA)', *Biomacromolecules*. <https://doi.org/10.1021/acs.biomac.8b01326>

[Link to publication on Research at Birmingham portal](#)

## **Publisher Rights Statement:**

This document is the unedited Author's version of a Submitted Work that was subsequently accepted for publication in *Biomacromolecules*, copyright © American Chemical Society after peer review. To access the final edited and published work see [10.1021/acs.biomac.8b01326](https://doi.org/10.1021/acs.biomac.8b01326)

## **General rights**

Unless a licence is specified above, all rights (including copyright and moral rights) in this document are retained by the authors and/or the copyright holders. The express permission of the copyright holder must be obtained for any use of this material other than for purposes permitted by law.

- Users may freely distribute the URL that is used to identify this publication.
- Users may download and/or print one copy of the publication from the University of Birmingham research portal for the purpose of private study or non-commercial research.
- User may use extracts from the document in line with the concept of 'fair dealing' under the Copyright, Designs and Patents Act 1988 (?)
- Users may not further distribute the material nor use it for the purposes of commercial gain.

Where a licence is displayed above, please note the terms and conditions of the licence govern your use of this document.

When citing, please reference the published version.

## **Take down policy**

While the University of Birmingham exercises care and attention in making items available there are rare occasions when an item has been uploaded in error or has been deemed to be commercially or otherwise sensitive.

If you believe that this is the case for this document, please contact [UBIRA@lists.bham.ac.uk](mailto:UBIRA@lists.bham.ac.uk) providing details and we will remove access to the work immediately and investigate.

## Article

**Poly(Sarcosine)-Based Nano-Objects with Multi-Protease Resistance by Aqueous Photoinitiated Polymerization-Induced Self-Assembly (Photo-PISA)**Spyridon Varlas, Panagiotis G. Georgiou, Panayiotis Bilalis,  
Joseph R. Jones, Nikos Hadjichristidis, and Rachel K. O'Reilly*Biomacromolecules*, **Just Accepted Manuscript** • DOI: 10.1021/acs.biomac.8b01326 • Publication Date (Web): 23 Oct 2018Downloaded from <http://pubs.acs.org> on October 29, 2018**Just Accepted**

"Just Accepted" manuscripts have been peer-reviewed and accepted for publication. They are posted online prior to technical editing, formatting for publication and author proofing. The American Chemical Society provides "Just Accepted" as a service to the research community to expedite the dissemination of scientific material as soon as possible after acceptance. "Just Accepted" manuscripts appear in full in PDF format accompanied by an HTML abstract. "Just Accepted" manuscripts have been fully peer reviewed, but should not be considered the official version of record. They are citable by the Digital Object Identifier (DOI®). "Just Accepted" is an optional service offered to authors. Therefore, the "Just Accepted" Web site may not include all articles that will be published in the journal. After a manuscript is technically edited and formatted, it will be removed from the "Just Accepted" Web site and published as an ASAP article. Note that technical editing may introduce minor changes to the manuscript text and/or graphics which could affect content, and all legal disclaimers and ethical guidelines that apply to the journal pertain. ACS cannot be held responsible for errors or consequences arising from the use of information contained in these "Just Accepted" manuscripts.



1  
2  
3  
4 Poly(Sarcosine)-Based Nano-Objects with Multi-  
5  
6  
7  
8  
9 Protease Resistance by Aqueous Photoinitiated  
10  
11  
12  
13 Polymerization-Induced Self-Assembly (Photo-  
14  
15  
16  
17 PISA)  
18  
19  
20  
21  
22

23 *Spyridon Varlas,<sup>a</sup> Panagiotis G. Georgiou,<sup>a,b</sup> Panayiotis Bilalis,<sup>c</sup> Joseph R. Jones,<sup>a</sup> Nikos*  
24 *Hadjichristidis,<sup>c\*</sup> and Rachel K. O'Reilly<sup>a\*</sup>*  
25  
26  
27

28  
29 <sup>a</sup> School of Chemistry, University of Birmingham, B15 2TT, Birmingham, UK

30  
31 <sup>b</sup> Department of Chemistry, University of Warwick, Gibbet Hill Road, CV4 7AL, Coventry, UK

32  
33 <sup>c</sup> Physical Sciences and Engineering Division, KAUST Catalysis Center, Polymer Synthesis  
34 Laboratory, King Abdullah University of Science and Technology (KAUST), 23955, Thuwal,  
35 Saudi Arabia  
36  
37  
38

39  
40 *\*Corresponding Authors:* nikolaos.hadjichristidis@kaust.edu.sa (N.H.) and  
41 r.oreilly@bham.ac.uk (R.K.O.R.)  
42  
43  
44  
45

46 KEYWORDS

47  
48 polymerization-induced self-assembly (PISA), ring-opening polymerization (ROP), reversible  
49 addition-fragmentation chain-transfer (RAFT) polymerization, photoinitiated polymerization,  
50  
51 poly(sarcosine), protease resistance.  
52  
53  
54  
55  
56  
57  
58  
59  
60

1  
2  
3 ABSTRACT  
4  
5  
6

7 Poly(sarcosine) (PSar) is a non-ionic hydrophilic poly(peptoid) with numerous biologically  
8 relevant properties, making it an appealing candidate for the development of amphiphilic block  
9 copolymer nanostructures. In this work, the fabrication of poly(sarcosine)-based diblock  
10 copolymer nano-objects with various morphologies *via* aqueous reversible addition-fragmentation  
11 chain-transfer (RAFT)-mediated photoinitiated polymerization-induced self-assembly (photo-  
12 PISA) is reported. Poly(sarcosine) was first synthesized *via* ring-opening polymerization (ROP)  
13 of sarcosine *N*-carboxyanhydride, using high-vacuum techniques. A small molecule chain transfer  
14 agent (CTA) was then coupled to the active  $\omega$ -amino chain end of the telechelic polymer for the  
15 synthesis of a poly(sarcosine)-based macro-CTA. Controlled chain-extensions of a commercially  
16 available water-miscible methacrylate monomer (2-hydroxypropyl methacrylate) were achieved  
17 *via* photo-PISA under mild reaction conditions, using PSar macro-CTA. Upon varying the degree  
18 of polymerization and concentration of the core-forming monomer, morphologies evolving from  
19 spherical micelles to worm-like micelles and vesicles were accessed, as determined by dynamic  
20 light scattering and transmission electron microscopy, resulting in the construction of a detailed  
21 phase diagram. The resistance of both colloiddally stable empty vesicles and enzyme-loaded  
22 nanoreactors against degradation by a series of proteases was finally assessed. Overall, our  
23 findings underline the potential of poly(sarcosine) as an alternative corona-forming polymer to  
24 poly(ethylene glycol)-based analogues of PISA assemblies for use in various pharmaceutical and  
25 biomedical applications.  
26  
27  
28  
29  
30  
31  
32  
33  
34  
35  
36  
37  
38  
39  
40  
41  
42  
43  
44  
45  
46  
47  
48  
49  
50  
51  
52  
53  
54  
55  
56  
57  
58  
59  
60

## INTRODUCTION

In modern polymer and materials science, poly(ethylene glycol) (PEG) and ethylene glycol-based polymers mainly from meth(acrylate) monomers are considered the gold standard for the design of nanostructures and materials with “stealth-like” properties.<sup>1-3</sup> PEG is widely utilized in various biotechnological applications such as drug/protein delivery and targeted diagnostics,<sup>4, 5</sup> surface coatings,<sup>6</sup> household and personal care products,<sup>7, 8</sup> and cell cryopreservation.<sup>9</sup> This is mainly attributed to the high flexibility and hydrophilicity, low cellular toxicity and biocompatible character of PEG that make it an efficient material for such applications.<sup>10</sup> However, PEG is known to be a non-bio-based and non-biodegradable polymer with limited functionality, while studies have also shown oxidative activity of PEG in physiological cellular environments, immune response of patients and accelerated blood clearance phenomena caused by anti-PEG antibodies.<sup>11-14</sup> Consequently, in recent years there is a growing demand for finding alternatives to overcome these limitations of PEG.<sup>15</sup>

A broad variety of hydrophilic polymers including poly(glycerols),<sup>16</sup> poly(oxazolines),<sup>17</sup> poly(peptides)<sup>18</sup> and poly(peptoids)<sup>19</sup> with comparable physicochemical properties to PEG have been currently explored and proposed as promising alternatives. Among them, poly(peptoids), an important family of biomaterials, only recently have attracted the attention of scientific community.<sup>19, 20</sup> Poly(sarcosine) (PSar), also referred as poly(*N*-methylated glycine), is the simplest member of the poly(peptoid) family that displays PEG-like properties and is based on an achiral endogenous but non-proteinogenic amino acid, sarcosine, mainly found in muscle tissues.<sup>21, 22</sup> N-Substitution of amino acid residues in poly(peptoids) is a common synthetic procedure to promote the random coil conformation over other secondary structures (e.g.  $\alpha$ -helices

1  
2  
3 and  $\beta$ -sheets) and to confer substantial flexibility to the polymer chains thus enhancing the  
4  
5 resistance of the derived materials toward enzymatic degradation.<sup>20, 23</sup> PSar is a non-ionic,  
6  
7 hydrophilic, highly biocompatible and potentially biodegradable polymer that exhibits low cellular  
8  
9 toxicity, limited interactions with blood components and “stealth-like” non-immunogenic  
10  
11 character.<sup>23, 24</sup> In addition to aqueous solubility, PSar is also highly soluble in common polar  
12  
13 organic solvents. Moreover, PSar can be synthesized *via* living ring-opening polymerization  
14  
15 (ROP) of the corresponding *N*-carboxyanhydride (NCA) to produce well-defined telechelic homo-  
16  
17 and copolymers with low dispersities.<sup>25, 26</sup> Further post-polymerization modification of the living  
18  
19 amino-terminal chain end allows for the insertion of various functionalities and the combination  
20  
21 of PSar with other synthetic polymers. Overall, the unique features of PSar suggest that it can be  
22  
23 effectively utilized as a PEG-alternative corona-forming block imparting higher colloidal stability  
24  
25 (i.e. prevention of protein-induced aggregation), minimal systemic toxicity and longer circulation  
26  
27 times *in vivo* to amphiphilic block copolymer assemblies.<sup>23</sup>  
28  
29  
30  
31  
32  
33

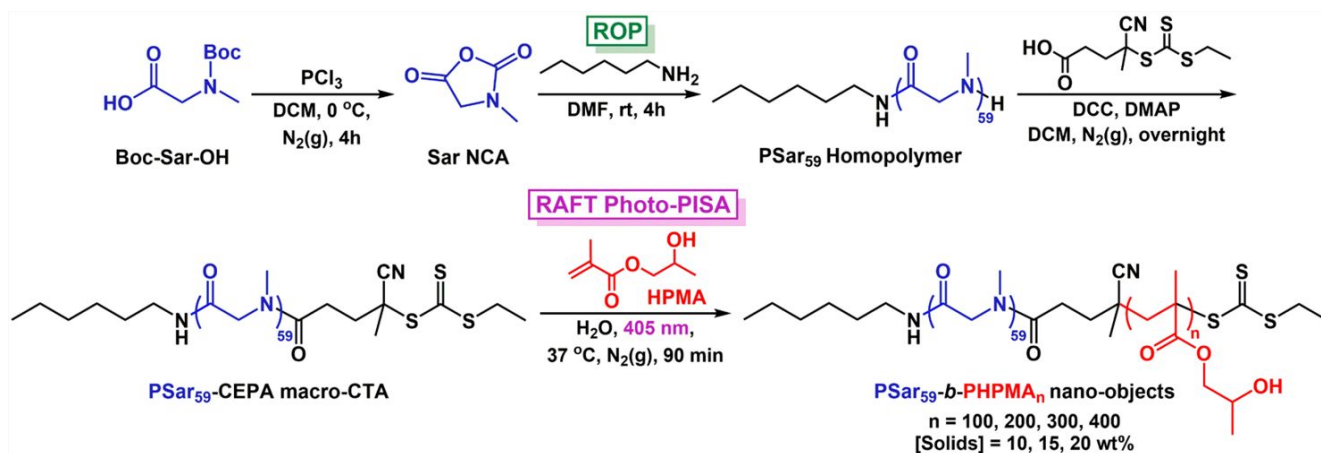
34 Over the last years, studies on the synthesis and self-assembly behavior of PSar-based block  
35  
36 copolymers for the development of nanostructures of biotechnological interest have been  
37  
38 presented, although they involve the use of conventional self-assembly procedures in dilute  
39  
40 aqueous solutions.<sup>13, 23, 27-32</sup> Recently, polymerization-induced self-assembly (PISA) has  
41  
42 been established as an efficient methodology for facile one-pot fabrication of polymeric  
43  
44 nano-objects with predictable morphologies at high solids concentrations (10-50% w/w).<sup>33-</sup>  
45  
46 <sup>36</sup> Existing limitations of traditional self-assembly strategies (i.e. direct dissolution, thin-  
47  
48 film hydration, and solvent-switch) such as low polymer concentrations ( $\leq 1\%$  w/w) and  
49  
50 laborious post-polymerization processing steps for targeting certain morphologies are  
51  
52 proven to be overcome by PISA. Only selected monomers have the ability to undergo PISA  
53  
54  
55  
56  
57  
58  
59  
60

1  
2  
3 since a solubility transition of the gradually growing core-forming block from solvent-  
4 soluble to solvent-immiscible is required.<sup>34</sup> In principle, PISA can be achieved by using  
5  
6 any known polymerization technique, although the vast majority of PISA studies to date  
7  
8 involve implementation of reversible-deactivation radical polymerization (RDRP)  
9  
10 techniques, including atom transfer radical polymerization (ATRP),<sup>37, 38</sup> nitroxide-  
11  
12 mediated polymerization (NMP),<sup>39, 40</sup> and reversible addition-fragmentation chain-transfer  
13  
14 (RAFT) polymerization,<sup>41-44</sup> under either dispersion or emulsion polymerization  
15  
16 conditions, owing to their versatility and broad applicability. Ring-opening metathesis  
17  
18 polymerization (ROMP) has been also introduced lately as a non-radical approach for PISA  
19  
20 in both aqueous and organic media.<sup>45-47</sup>  
21  
22  
23  
24  
25  
26

27 In particular, there has been rapidly growing research interest in aqueous RAFT-mediated  
28  
29 photoinitiated PISA (photo-PISA) *via* either the well-described “photoiniferter”  
30  
31 mechanism of chain transfer agents (CTAs) or by using special photoinitiators and  
32  
33 photoredox catalysts under ultraviolet or visible-light irradiation.<sup>42, 48-54</sup> This is mainly  
34  
35 attributed to the ambient temperatures and mild reaction conditions of photo-PISA that are  
36  
37 not harmful to sensitive biomolecules (i.e. drugs, enzymes, membrane proteins) enabling  
38  
39 their direct encapsulation into well-defined polymeric vesicles for the one-pot development  
40  
41 of cargo-loaded delivery vehicles and nanoreactors of further bio-related interest.<sup>55-59</sup>  
42  
43  
44  
45

46 Herein, the preparation of diblock copolymer nano-objects with different morphologies bearing  
47  
48 a PSar hydrophilic corona *via* a combination of NCA ROP and RAFT-mediated photo-PISA is  
49  
50 reported. First, sarcosine NCA (Sar NCA) was synthesized from the corresponding *N*-Boc-  
51  
52 protected amino acid. Living ROP of Sar NCA using high-vacuum techniques and an amino  
53  
54 initiator yielded an  $\omega$ -telechelic PSar homopolymer with monomodal molecular weight  
55  
56  
57  
58  
59  
60

distribution and low dispersity ( $D_M$ ). Due to the absence of side chain functional groups found in poly(peptides), quantitative coupling between an acid-functionalized small molecule CTA and the sterically accessible N-terminus of PSar was achieved, resulting in the formation of a water-soluble PSar macromolecular CTA (macro-CTA). As a next step, PSar macro-CTA was used to carry out aqueous photo-PISA reactions of 2-hydroxypropyl methacrylate (HPMA) under dispersion polymerization conditions by varying PHPMA degrees of polymerization and total solids concentration (Scheme 1). The obtained PSar-*b*-PHPMA diblock copolymer assemblies were characterized by dynamic light scattering (DLS), zeta-potential analysis and transmission electron microscopy (TEM) imaging, resulting in the construction of a morphologies diagram. To further explore the robust nature and PEG-like characteristics of PSar-based nano-objects, the colloidal stability of PSar-*b*-PHPMA unilamellar vesicles in physiological media and the effect of a series of typical proteolytic enzymes (i.e.  $\alpha$ -chymotrypsin, trypsin and pepsin) on empty and protein-loaded vesicles were evaluated revealing the great potential of such materials for biomedical applications.



**Scheme 1.** Schematic illustration of the synthetic route followed for the synthesis of PSar<sub>59</sub>-*b*-PHPMA<sub>n</sub> ( $n = 100, 200, 300, \text{ and } 400$ ) diblock copolymer nano-objects at [solids] = 10, 15, and 20 wt% *via* aqueous RAFT-mediated photo-PISA, using a PSar<sub>59</sub>-based macro-CTA.



## EXPERIMENTAL SECTION

### Materials and methods

Materials and characterization techniques used are given in detail in the Supporting Information (SI).

### Synthetic Procedures

**Synthesis of sarcosine *N*-carboxyanhydride (Sar NCA).** Boc-*N*-methylglycine (Boc-Sar-OH) (7.0 g, 0.037 mol) was added into a three-neck round-bottom flask and degassed under vacuum overnight. Then, 300 mL of dry DCM was distilled and the solution was left under stirring for 30 min at 0 °C. Subsequently, phosphorous trichloride (PCl<sub>3</sub>) (4.0 mL, 0.046 mol) was diluted into 30 mL of dry DCM, added dropwise to the flask *via* a dropping funnel and the reaction was left to proceed for 4 h at 0 °C under nitrogen atmosphere. The solvent and the volatiles were removed under reduced pressure, yielding a yellowish oil as the crude reaction product. The crude product was then sublimated at 70 °C under high vacuum (10<sup>-5</sup> mbar) resulting in the formation of Sar NCA crystals (3.1 g, 0.027 mol, 73%, m. p.: 103–104 °C (lit.: 102–105 °C)).<sup>60</sup> <sup>1</sup>H-NMR (400 MHz, DMSO-*d*<sub>6</sub>): δ (ppm) 4.23 (s, 2H, **CH**<sub>2</sub>), 2.87 (s, 3H, **CH**<sub>3</sub>). FT-IR (neat): ν (cm<sup>-1</sup>) 1848, 1761 (C=O).

**Synthesis of 4-cyano-4-[(ethylsulfanylthiocarbonyl)sulfanyl] pentanoic acid (CEPA).** A previously described process was followed for the synthesis of 4-cyano-4-[(ethylsulfanylthiocarbonyl)sulfanyl] pentanoic acid chain transfer agent (CEPA CTA).<sup>61</sup> In

1  
2  
3 particular, sodium ethanethiolate (10.0 g, 0.119 mol, 1 eq) was suspended in 500 mL of dry diethyl  
4 ether at 0 °C. Carbon disulfide (7.74 mL, 0.131 mol, 1.1 eq) was subsequently added dropwise  
5  
6 over 10 min, resulting to the formation of a thick yellow precipitate of sodium *S*-ethyl  
7  
8 trithiocarbonate. After 2 h of stirring at room temperature, solid iodine (15.1 g, 0.059 mol, 0.5 eq)  
9  
10 was added to the reaction medium. After 2 h, the solution was washed three times with aqueous  
11  
12 sodium thiosulfate (1 M), water and finally saturated NaCl solution. The organic layer was  
13  
14 thoroughly dried over MgSO<sub>4</sub> and the crude bis-(ethylsulfanylthiocarbonyl) disulfide was then  
15  
16 isolated by rotary evaporation (16.2 g, 0.059 mol).  
17  
18

19  
20 A solution of bis-(ethylsulfanylthiocarbonyl) disulfide (16.2 g, 0.059 mol, 1 eq) and 4,4'-azobis(4-  
21  
22 cyanopentanoic acid) (ACVA) (24.8 g, 0.0885 mol, 1.5 eq) in 500 mL ethyl acetate was heated at  
23  
24 reflux for 18 h under N<sub>2</sub>(g) atmosphere. Following rotary evaporation of the solvent, the crude  
25  
26 CEPA CTA was isolated by flash column chromatography using silica gel as the stationary phase  
27  
28 and 75:25 DCM-petroleum ether as the eluent. The isolated product was precipitated out of  
29  
30 solution using hexane, leaving a yellow-light orange solid. The final product was collected and  
31  
32 dried under reduced pressure to afford pure CEPA CTA (21.36 g, 0.081 mol, 69%). <sup>1</sup>H-NMR (400  
33  
34 MHz, CDCl<sub>3</sub>): δ (ppm) 3.35 (q, 2H, S-CH<sub>2</sub>-CH<sub>3</sub>), 2.38-2.71 (m, 4H, CH<sub>2</sub>-CH<sub>2</sub>), 1.89 (s, 3H,  
35  
36 C(CN)-CH<sub>3</sub>), 1.36 (t, 3H, S-CH<sub>2</sub>-CH<sub>3</sub>). <sup>13</sup>C-NMR (100 MHz, CDCl<sub>3</sub>): δ (ppm) 217.0, 177.2,  
37  
38 119.2, 46.5, 33.5, 31.7, 29.5, 25.0, 12.9. FT-IR (neat): ν (cm<sup>-1</sup>) 2235 (C≡N), 1709 (C=O), 1073  
39  
40 (C=S). HRMS: m/z [C<sub>9</sub>H<sub>13</sub>NO<sub>2</sub>S<sub>3</sub>+Na]<sup>+</sup> calc. 286.0001 g mol<sup>-1</sup>, exp. 286.0001 g mol<sup>-1</sup>.  
41  
42  
43  
44  
45  
46  
47  
48  
49

### 50 **Synthesis of poly(sarcosine)<sub>59</sub> (PSar<sub>59</sub>) via ring-opening polymerization (ROP) of Sar NCA.**

51  
52 In a flame-dried round bottom flask, n-hexylamine (0.048 mL, 3.6×10<sup>-5</sup> mol) was added, followed  
53  
54 by distillation of 30 mL highly pure DMF. The flask was transferred to the glove box and a 10 mL  
55  
56  
57  
58  
59  
60

1  
2  
3 solution of Sar NCA (2.9 g, 0.0252 mol) in DMF was added and the solution was vigorously stirred  
4  
5 at room temperature. Periodically, the solution was pumped to remove the CO<sub>2</sub> (g) produced  
6  
7 during polymerization. The consumption of Sar NCA was monitored by FT-IR spectroscopy  
8  
9 through removal of an aliquot of the solution in the glove box. Upon completion of the  
10  
11 polymerization reaction (4 h), the final PSar homopolymer was precipitated in diethyl ether and  
12  
13 dried under vacuum overnight (1.5 g, 83%). <sup>1</sup>H-NMR (400 MHz, D<sub>2</sub>O): δ (ppm) 4.49-4.05 (br m,  
14  
15 CH<sub>2</sub> of PSar backbone), 3.21 (m, 2H, CH<sub>2</sub>-CH<sub>2</sub>-NH), 3.10-2.81 (br m, CH<sub>3</sub> of PSar side chain),  
16  
17 1.50 (s, 2H, (CH<sub>2</sub>)<sub>3</sub>-CH<sub>2</sub>-CH<sub>2</sub>-NH), 1.29 (s, 6H, CH<sub>3</sub>-(CH<sub>2</sub>)<sub>3</sub>-CH<sub>2</sub>), 0.86 (s, 3H, CH<sub>3</sub>-(CH<sub>2</sub>)<sub>3</sub>-CH<sub>2</sub>).  
18  
19  $M_{n, \text{NMR}} = 4,200 \text{ g mol}^{-1}$  ( $DP_{\text{PSar, NMR}} = 59$ ). FT-IR (neat): ν (cm<sup>-1</sup>) 1641 (C=O of amide). SEC (5  
20  
21 mM NH<sub>4</sub>BF<sub>4</sub> in DMF)  $M_{n, \text{SEC RI}} = 7,700 \text{ g mol}^{-1}$ ,  $D_{M, \text{SEC RI}} = 1.08$ .  $M_{w, \text{SLS}} = 5,500 \text{ g mol}^{-1}$ .  
22  
23  
24  
25  
26  
27  
28

29 **Synthesis of poly(sarcosine)<sub>59</sub>-CEPA macro-CTA (PSar<sub>59</sub>-CEPA macro-CTA).** PSar<sub>59</sub>-CEPA  
30  
31 macro-CTA was synthesized by dicyclohexylcarbodiimide (DCC) coupling between PSar<sub>59</sub> and  
32  
33 CEPA CTA according to previously reported methods.<sup>42, 48, 59</sup> Poly(sarcosine) homopolymer ( $M_{n, \text{NMR}} = 4,200 \text{ g mol}^{-1}$ , PSar<sub>59</sub>) (1 g,  $2.4 \times 10^{-4}$  mol, 1 eq) was dissolved in 20 mL of dry DCM. The  
34  
35 resulting solution was then purged with N<sub>2</sub> (g) for 30 min. After complete dissolution, CEPA CTA  
36  
37 (0.253 g,  $9.6 \times 10^{-4}$  mol, 4 eq), DCC (99 mg,  $4.8 \times 10^{-4}$  mol, 2 eq) and DMAP (5.9 mg,  $4.8 \times 10^{-5}$  mol,  
38  
39 0.2 eq) were added to the reaction mixture. The amide formation reaction proceeded with stirring  
40  
41 at room temperature for 18 h under continuous N<sub>2</sub> (g) flow. After this period, DCC (99 mg,  $4.8 \times 10^{-4}$   
42  
43 mol, 2 eq) and DMAP (5.9 mg,  $4.8 \times 10^{-5}$  mol, 0.2 eq) were added for a second time to the reaction  
44  
45 mixture and then stirred at room temperature for an additional period of 6 h under continuous N<sub>2</sub>  
46  
47 (g) flow. The solution was then filtered to remove unreacted DCC and DMAP. Following rotary  
48  
49 evaporation of DCM, the resulted PSar<sub>59</sub>-CEPA macro-CTA was collected by precipitation into  
50  
51  
52  
53  
54  
55  
56  
57  
58  
59  
60

1  
2  
3 250 mL of cold diethyl ether, redissolved in deionized water (DI) and dialyzed against DI water  
4  
5 for 48 h (dialysis membrane MWCO = 1,000 Da). The purified PSar<sub>59</sub>-CEPA macro-CTA was  
6  
7 then lyophilized to give a yellowish solid as the final product (0.82 g,  $1.8 \times 10^{-4}$  mol, 76%). <sup>1</sup>H-  
8  
9 NMR (400 MHz, CDCl<sub>3</sub>):  $\delta$  (ppm) 4.35-3.85 (br m, CH<sub>2</sub> of PSar backbone), 3.35 (q, 2H, CH<sub>3</sub>-  
10  
11 CH<sub>2</sub>-S-(C=S)), 3.21 (m, 2H, CH<sub>2</sub>-CH<sub>2</sub>-NH), 3.10-2.85 (br m, CH<sub>3</sub> of PSar side chain), 2.69 (m,  
12  
13 2H, CH<sub>2</sub>-(C=O)-N-CH<sub>3</sub>), 2.52-2.35 (m, 2H, C(CN)-CH<sub>2</sub>), 1.91 (s, 3H, CH<sub>3</sub>-C-(CN)), 1.49 (s, 2H,  
14  
15 (CH<sub>2</sub>)<sub>3</sub>-CH<sub>2</sub>-CH<sub>2</sub>-NH), 1.36 (t, 3H, CH<sub>3</sub>-CH<sub>2</sub>-S-(C=S)), 1.25 (d, 6H, CH<sub>3</sub>-(CH<sub>2</sub>)<sub>3</sub>-CH<sub>2</sub>), 0.88 (s,  
16  
17 3H, CH<sub>3</sub>-(CH<sub>2</sub>)<sub>3</sub>-CH<sub>2</sub>). SEC (5 mM NH<sub>4</sub>BF<sub>4</sub> in DMF)  $M_{n, SEC RI} = 8,300 \text{ g mol}^{-1}$ ,  $D_{M, SEC RI} = 1.09$ .  
18  
19  
20  
21  
22  
23

#### 24 **Synthesis of PSar<sub>59</sub>-*b*-PHPMA<sub>n</sub> diblock copolymer nano-objects by aqueous RAFT-mediated**

25 **photoinitiated polymerization-induced self-assembly (photo-PISA).** All photo-PISA reactions

26  
27 were performed in a custom-built photoreactor setup (see the Supporting Information for details).  
28  
29

30 This ensured the polymerization solutions were only exposed to the light from the 400–410 nm  
31  
32

33 LED source placed underneath the vials (radiant flux of 800 mW@400 mA). A typical synthetic  
34  
35

36 procedure to achieve PSar<sub>59</sub>-*b*-PHPMA<sub>200</sub> diblock copolymer nano-objects at 15 wt% solids  
37  
38

39 content by aqueous RAFT-mediated photo-PISA is described.<sup>42, 59</sup> PSar<sub>59</sub>-CEPA mCTA (20 mg,  
40  
41

42  $4.4 \times 10^{-6}$  mol, 1 eq) and HPMA (128 mg,  $8.9 \times 10^{-4}$  mol, 200 eq) were dissolved in deionized water  
43  
44

45 (0.84 mL) in a sealed 15 mL scintillation vial bearing a magnetic stirrer bar. The resulting  
46  
47

48 polymerization solution was degassed by purging with N<sub>2</sub> (g) for 15 min. The sealed vial was  
49  
50

51 incubated at 37 °C with magnetic stirring under 405 nm light irradiation for 90 min to ensure full  
52  
53

54 monomer conversion. After this period, the reaction mixture was exposed to air and allowed to  
55  
56

57 cool to room temperature. The resulting solution of particles was then diluted ten-fold in DI water  
58  
59

60 and purified by three centrifugation/resuspension cycles in DI water at 14000 rpm. <sup>1</sup>H-NMR in

1  
2  
3 methanol- $d_4$  and DMF SEC analyses of the pure copolymers were performed after lyophilization  
4 of an aliquot of particles. TEM, DLS and zeta potential analyses were performed on samples after  
5 dilution to an appropriate analysis concentration.  $^1\text{H-NMR}$  (400 MHz,  $\text{CD}_3\text{OD}$ ):  $\delta$  (ppm) 5.60 (br  
6 s,  $\text{OH}$ ), 4.47-4.10 (br m,  $\text{CH}_2$  of PSar backbone), 4.03 and 3.88 (br s,  $\text{CH}$  and  $\text{CH}_2$  of PHPMA  
7 side chain), 3.63 (br s,  $\text{CH}$  of PHPMA side chain, isomer peak), 3.10-2.89 (br m,  $\text{CH}_3$  of PSar side  
8 chain), 2.23-1.75 (br m,  $\text{CH}_2$  of PHPMA backbone), 1.50-0.75 (br m,  $\text{CH}_3$  of PHPMA backbone  
9 and  $\text{CH}_3$  of PHPMA side chain).  
10  
11  
12  
13  
14  
15  
16  
17  
18  
19  
20  
21

22 **Encapsulation of HRP into PSar<sub>59</sub>-*b*-PHPMA<sub>400</sub> vesicles by one-pot aqueous RAFT photo-**  
23 **PISA.** For the preparation of HRP-loaded PSar<sub>59</sub>-*b*-PHPMA<sub>400</sub> vesicles by aqueous photo-PISA at  
24 10 wt% solids content, a typical synthetic protocol was followed.<sup>57</sup> PSar<sub>59</sub>-CEPA mCTA (10 mg,  
25  $2.2 \times 10^{-6}$  mol, 1 eq) and HPMA (128 mg,  $8.9 \times 10^{-4}$  mol, 400 eq) were dissolved in deionized water  
26 (1.14 mL) in a sealed 15 mL scintillation vial bearing a magnetic stirrer bar. Once homogeneous,  
27 0.1 mL of a 200 U mL<sup>-1</sup> HRP solution in DI water was added. The resulting polymerization  
28 solution was degassed by purging with N<sub>2</sub> (g) for 15 min. The sealed vial was incubated at 37 °C  
29 with magnetic stirring under 405 nm light irradiation for 90 min to ensure full monomer  
30 conversion. After this period, the reaction mixture was exposed to air and allowed to cool to room  
31 temperature. The resulting solution of particles was then diluted ten-fold in 100 mM PB (pH = 7.0)  
32 and purified by five centrifugation/resuspension cycles in 100 mM PB (pH = 7.0) at 14000 rpm  
33 for the removal of unreacted monomer and free HRP enzyme.  
34  
35  
36  
37  
38  
39  
40  
41  
42  
43  
44  
45  
46  
47  
48  
49  
50  
51  
52

53 **Incubation of empty and HRP-loaded PSar<sub>59</sub>-*b*-PHPMA<sub>400</sub> vesicles with different proteolytic**  
54 **enzymes (proteases).** Empty PSar<sub>59</sub>-*b*-PHPMA<sub>400</sub> vesicles purified in 100 mM phosphate buffer  
55  
56  
57  
58  
59  
60

(PB) (pH = 7.0 for a-chymotrypsin and trypsin or pH = 1.8 for pepsin) at 10× dilution (1 wt% solids content) (2 mL) were incubated with either 25 mg mL<sup>-1</sup> a-CT (pH = 7.0), 25 mg mL<sup>-1</sup> trypsin (pH = 7.0) or 25 mg mL<sup>-1</sup> pepsin (pH = 1.8) solutions (0.2 mL) at 37 °C. Aliquots were taken over a period of 72 h and samples were analyzed by DLS, DMF SEC and dry-state TEM imaging to determine the effect of different proteases on the characteristics of particles.

HRP-loaded PSar<sub>59</sub>-*b*-PHPMA<sub>400</sub> vesicles purified in 100 mM PB (pH = 7.0 for a-CT and trypsin) at 10× dilution (1 wt% solids content) (2 mL) were incubated with either 100 mM PB (pH = 7.0), 25 mg mL<sup>-1</sup> a-CT or trypsin (pH = 7.0) solutions (0.2 mL) at 37 °C for a period of 72 h. Aliquots were taken at 18 h and 72 h and the relative activities of particles were assessed by kinetic colorimetric analysis using a plate reader. For the free HRP, 2 U mL<sup>-1</sup> solutions in 100 mM PB (pH = 7.0) (2 mL) were incubated with either 100 mM PB (pH = 7.0), 25 mg mL<sup>-1</sup> a-CT or trypsin (pH = 7.0) solutions (0.2 mL) at 37 °C for a period of 72 h. Aliquots were taken at 18 h and 72 h and the relative activities of free HRP solutions were assessed in an identical manner. Pepsin was not used in case of HRP-loaded vesicles due to significant difference in optimum pH range of the two enzymes.

**Kinetic colorimetric analyses for determination of activity of HRP-loaded PSar<sub>59</sub>-*b*-PHPMA<sub>400</sub> vesicles in presence of different proteases.** Purified HRP-loaded PSar<sub>59</sub>-*b*-PHPMA<sub>400</sub> vesicles incubated with either PB, a-CT or trypsin at 20× dilution (0.5 wt% solids content) in 100 mM PB (pH = 7.0) (120 μL) were diluted with 100 mM PB (pH = 7.0) (40 μL) in a 96-well plate microwell. *O*-dianisidine (4 mM, 20 μL) was then added. Finally, a 35 wt% aqueous solution of hydrogen peroxide (20 μL) was added and the change in absorbance at λ = 492 nm was recorded every minute for a period of 60 min using a plate reader. In a similar process, the free

1  
2  
3 HRP solutions incubated with either PB, a-CT or trypsin at  $1 \text{ U mL}^{-1}$  in  $100 \text{ mM PB (pH = 7.0)}$   
4  
5  $(20 \text{ }\mu\text{L})$  were diluted with  $100 \text{ mM PB (pH = 7.0)}$   $(140 \text{ }\mu\text{L})$  in a 96-well plate microwell. *O*-  
6  
7 dianisidine  $(4 \text{ mM}, 20 \text{ }\mu\text{L})$  was then added. Finally, a  $35 \text{ wt}\%$  aqueous solution of hydrogen  
8  
9 peroxide  $(20 \text{ }\mu\text{L})$  was added and the change in absorbance was monitored in an identical manner.  
10  
11  
12 All measurements were performed in quadruplicate.  
13  
14  
15  
16

17 **Colloidal stability studies of PSar<sub>59</sub>-*b*-PHPMA<sub>400</sub> vesicles in physiological media.** To assess  
18  
19 the colloidal stability of empty PSar<sub>59</sub>-*b*-PHPMA<sub>400</sub> vesicles (prepared at  $[\text{solids}] = 10 \text{ wt}\%$ ) and  
20  
21 their interaction with complex physiological media, a typical protocol was followed.<sup>62</sup> FBS and  
22  
23 cell growth medium were first incubated at  $37 \text{ }^\circ\text{C}$  for 15 min. Purified PSar<sub>59</sub>-*b*-PHPMA<sub>400</sub> vesicles  
24  
25 were suspended in DI water at a final concentration of  $1 \text{ wt}\%$  prior to mixing with FBS or cell  
26  
27 growth medium. Then,  $80 \text{ }\mu\text{L}$  of  $1 \text{ wt}\%$  vesicles were dispersed in either  $10 \text{ mL DI water}$  or cell  
28  
29 growth medium or  $10 \text{ mL}$  of  $1:9 \text{ FBS:DI H}_2\text{O}$  solution, with gentle agitation. The resulting particle  
30  
31 solutions were incubated at  $37 \text{ }^\circ\text{C}$  and  $D_h$  changes of vesicles were monitored by DLS over a period  
32  
33 of 72 h.  
34  
35  
36  
37  
38  
39

## 40 RESULTS AND DISCUSSION

41  
42 **Synthesis and characterization of poly(sarcosine)<sub>59</sub> (PSar<sub>59</sub>) homopolymer.** The first  
43  
44 step for the preparation of PSar homopolymer involved the synthesis of the corresponding  
45  
46 *N*-carboxyanhydride of sarcosine (Sar NCA). This was achieved by cyclization reaction of  
47  
48 *N*-Boc-protected sarcosine using  $\text{PCl}_3$  as chlorinating agent for the formation of Sar NCA  
49  
50 ring molecule (Scheme 1). The reaction was completed in 4 h as evidenced by FT-IR  
51  
52 spectroscopy (Figure S2, SI). The appearance of two characteristic peaks at 1761 and 1848  
53  
54  
55  
56  
57  
58  
59  
60

1  
2  
3 cm<sup>-1</sup> are indicative of the  $\nu(\text{C}=\text{O})$  vibrations of the Sar NCA ring. The crude product was  
4 purified by sublimation *in vacuo* resulting in the formation of Sar NCA crystals. The  
5  
6 successful synthesis and purification of Sar NCA was confirmed by <sup>1</sup>H-NMR spectroscopy  
7  
8 in DMSO-*d*<sub>6</sub> (Figure S1A, SI). Although the “Fuchs-Farthing” method is considered the  
9  
10 standard approach for the synthesis of amino acid NCAs (i.e. use of phosgene or derivatives  
11  
12 at elevated temperatures), the alternative mild synthetic procedure followed herein resulted  
13  
14 in highly pure final product of Sar NCA at high yield.  
15  
16  
17  
18

19  
20 Next,  $\omega$ -telechelic PSar homopolymer was synthesized *via* living ring-opening  
21  
22 polymerization (ROP) of Sar NCA. The polymerization reaction proceeded under high  
23  
24 vacuum at room temperature for 4 h using n-hexylamine as the initiator and DMF as the  
25  
26 solvent, and was terminated by precipitation in diethylether (Scheme 1). Monitoring of the  
27  
28 ROP kinetics was carried out *via* FT-IR spectroscopy as evidenced by the disappearance of  
29  
30 the NCA peaks (1761 and 1848 cm<sup>-1</sup>) and the gradual appearance of a sharp peak at 1641  
31  
32 cm<sup>-1</sup> attributed to the  $\nu(\text{C}=\text{O})$  vibration of the formed poly(peptoid) amide bonds (Figure  
33  
34 S2, SI). SEC analysis in DMF with 5 mM NH<sub>4</sub>BF<sub>4</sub> was carried out to get a rough molecular  
35  
36 weight estimate of the homopolymer as PMMA can be poor standard for PSar, while it  
37  
38 revealed a narrow monomodal molecular weight distribution peak of low dispersity ( $M_n$ ,  
39  
40  $SEC_{RI} = 7,700 \text{ g mol}^{-1}$ ,  $D_{MRI} = 1.08$ ) (Figure 1B).<sup>60</sup> <sup>1</sup>H-NMR spectroscopy in D<sub>2</sub>O was used  
41  
42 for the determination of the average degree of polymerization (DP) of the final purified  
43  
44 PSar by comparing the integral ratio of the peak corresponding to -CH<sub>3</sub> group of  
45  
46 hexylamine at 0.86 ppm ( $I_{0.86 \text{ ppm}} = 3.00$ ) to the peak of -CH<sub>3</sub> groups of PSar backbone at  
47  
48 2.81-3.10 ppm ( $I_{2.81-3.10 \text{ ppm}} = 177.25$ ) (ca.  $DP_{PSar} = 59$ ,  $M_{n, NMR} = 4,200 \text{ g mol}^{-1}$ ) (Figure S1B,  
49  
50 SI). Analysis of static and dynamic light scattering over a range of scattering lengths (10.7  
51  
52  
53  
54  
55  
56  
57  
58  
59  
60



$\leq q \leq 23.0 \mu\text{m}^{-1}$ ) was used to estimate the weight-average molecular weight and intensity-weighted hydrodynamic radius of PSar<sub>59</sub> in DI water ( $M_w = (5.50 \pm 0.09) \times 10^3 \text{ Da}$ ;  $\langle R_h \rangle_Z = (1.95 \pm 0.03) \text{ nm}$ ) (Figure S3, SI). The mutual consistency of these two measurements was then verified by reference to an empirical formula published previously by Weber et al.<sup>60</sup>

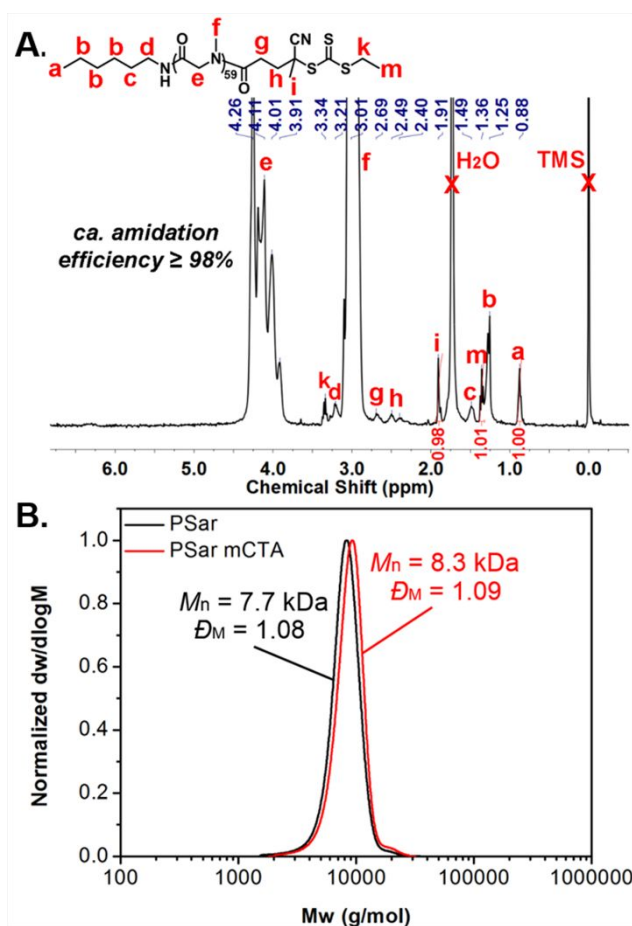


**Figure 1.** (A)  $^1\text{H}$ -NMR spectrum of PSar<sub>59</sub>-CEPA macro-CTA in  $\text{CDCl}_3$ . (B) Normalized SEC RI molecular weight distributions for PSar<sub>59</sub> homopolymer (black trace) and PSar<sub>59</sub>-CEPA macro-CTA (red trace), along with the corresponding  $M_n$  and  $D_M$  values.  $M_n$  and  $D_M$  values were calculated from PMMA standards using 5 mM  $\text{NH}_4\text{BF}_4$  in DMF as the eluent.

**Aqueous RAFT-mediated photoinitiated polymerization-induced self-assembly (photo-PISA) of PSar<sub>59</sub>-*b*-PHPMA<sub>n</sub> diblock copolymer nano-objects.** In order to conduct aqueous RAFT-mediated photo-PISA reactions using PSar<sub>59</sub> as the hydrophilic steric stabilizer, a small molecule CTA (CEPA CTA) suitable for methacrylate monomers was introduced to the PSar chain ends to afford a PSar-based macro-CTA. This was achieved through amide bond formation between the acid-functionalized CEPA CTA and the sterically accessible amino end group of PSar by DCC coupling chemistry under dry conditions (Scheme 1). Quantitative amidation efficiency ( $\geq 98\%$ ) was calculated from <sup>1</sup>H-NMR spectroscopy in chloroform-*d* by comparing the integral ratio of the peak corresponding to –CH<sub>3</sub> group of hexylamine at 0.88 ppm ( $I_{0.88 \text{ ppm}} = 1.00$ ) to the peak of –CH<sub>3</sub> group of CTA at 1.91 ppm ( $I_{1.91 \text{ ppm}} = 0.98$ ) (ca. amidation efficiency (%) =  $(I_{1.91 \text{ ppm}}/I_{0.88 \text{ ppm}}) \times 100$ , Figure 1A). Based on <sup>1</sup>H-NMR analysis, there is approximately 2% of non-functionalized PSar<sub>59</sub> homopolymer that is not separated from PSar<sub>59</sub>-CEPA macro-CTA as they both precipitate from diethyl ether. SEC analysis of the purified and lyophilized PSar<sub>59</sub> macro-CTA in 5 mM NH<sub>4</sub>BF<sub>4</sub> in DMF revealed the successful attachment of CEPA, as judged by the small increase of molecular weight compared to PSar<sub>59</sub> and the characteristic absorbance of the trithiocarbonate group of the macro-CTA peak at  $\lambda = 309 \text{ nm}$  ( $M_{n, \text{SEC RI}} = 8,300 \text{ g mol}^{-1}$ ,  $D_{\text{M RI}} = 1.09$ ) (Figure 1B).

Subsequently, the prepared water-soluble PSar<sub>59</sub> macro-CTA was chain-extended under RAFT dispersion PISA conditions using the well-documented water-miscible monomer 2-hydroxypropyl methacrylate (HPMA) (mixture of 2-hydroxypropyl methacrylate - 75 mol % and 2-hydroxyisopropyl methacrylate – 25 mol%) for the formation of the water-insoluble core-forming block. Aqueous RAFT-mediated photo-PISA reactions of HPMA for the fabrication of PSar<sub>59</sub>-*b*-PHPMA<sub>n</sub> diblock copolymer nano-objects were carried out under 405

1  
2  
3 nm visible-light irradiation (radiant flux of 800 mW@400 mA) at 37 °C (N<sub>2</sub> atmosphere) in  
4  
5 the absence of a photoinitiator or catalyst (Scheme 1). As an initial step, the required photo-  
6  
7 PISA reaction time to ensure complete monomer conversions was determined *via* kinetic  
8  
9 study of a PSar<sub>59</sub>-*b*-PHPMA<sub>400</sub> system at 10 wt% total solids content. Aliquots were  
10  
11 withdrawn from the polymerization mixture every 5 min and samples were analysed by <sup>1</sup>H-  
12  
13 NMR spectroscopy in methanol-*d*<sub>4</sub> for monomer conversion calculation and SEC analysis  
14  
15 using 5 mM NH<sub>4</sub>BF<sub>4</sub> in DMF as the eluent. As shown in Figure 2A, the photo-PISA reaction  
16  
17 followed pseudo-first-order kinetics separated into two regimes with quantitative monomer  
18  
19 conversion (>99%) achieved after 90 min of irradiation time. Based on the semilogarithmic  
20  
21 plot, the first regime from 0 to 25 min corresponds to growing solvent-soluble PSar<sub>59</sub>-*b*-  
22  
23 PHPMA<sub>n</sub> chains, while for the second regime a significant increase in polymerization rate  
24  
25 typically occurring in a PISA process was observed after approximately 25 min ascribed to a  
26  
27 monomer conversion of 36.5% that is attributed to the onset of particle micellization resulting  
28  
29 in a relatively high local HPMA concentration.<sup>33, 63</sup> SEC monitoring during the kinetic study  
30  
31 revealed the linear evolution of *M*<sub>n</sub> values with conversion and verified the controlled  
32  
33 character of the photo-PISA process, while *D*<sub>M</sub> values remained relatively low with  
34  
35 progression of conversion (*D*<sub>M</sub> max = 1.50), given that a high DP of PHPMA was targeted in  
36  
37 this case (Figure 2B).  
38  
39  
40  
41  
42  
43  
44  
45  
46  
47  
48  
49  
50  
51  
52  
53  
54  
55  
56  
57  
58  
59  
60

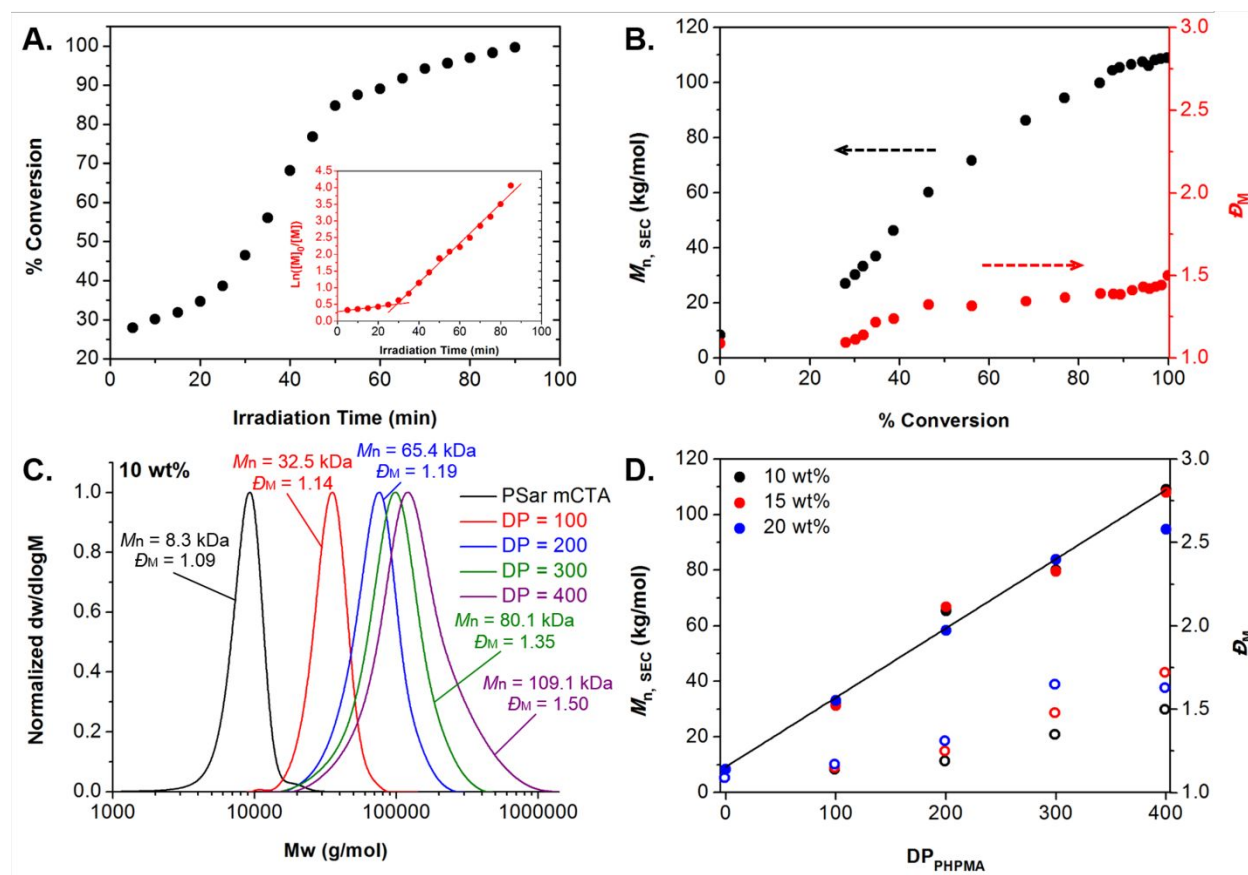


**Figure 2.** (A) Polymerization kinetics for aqueous RAFT-mediated photo-PISA of HPMA using PSar<sub>59</sub>-CEPA as the macro-CTA at [solids] = 10 wt% (target DP<sub>PHPMA</sub> = 400) (inset:  $\ln([M]_0/[M])$  versus irradiation time kinetic plot). (B) Evolution of number-average molecular weight ( $M_n$ ) and molar mass distribution ( $\mathcal{D}_M$ ) values with monomer conversion for aqueous RAFT-mediated photo-PISA of HPMA using PSar<sub>59</sub>-CEPA as the macro-CTA at [solids] = 10 wt% (target DP<sub>PHPMA</sub> = 400). (C) Normalized SEC RI molecular weight distributions for PSar<sub>59</sub>-CEPA macro-CTA (black trace) and PSar<sub>59</sub>-*b*-PHPMA<sub>n</sub> diblock copolymers (n = 100 - red trace, 200 - blue trace, 300 - green trace, and 400 - purple trace) at [solids] = 10 wt%, along with their corresponding  $M_n$  and  $\mathcal{D}_M$  values. (D) Evolution of  $M_n$  (filled circles) and  $\mathcal{D}_M$  (empty circles) values calculated from SEC RI analysis with increasing target DP of PHPMA for PSar<sub>59</sub>-*b*-PHPMA<sub>n</sub> diblock copolymers prepared *via* aqueous RAFT-mediated photo-PISA at [solids] = 10, 15, and 20 wt%. In all cases  $M_n$  and  $\mathcal{D}_M$  values were calculated from PMMA standards using 5 mM NH<sub>4</sub>BF<sub>4</sub> in DMF as the eluent.

1  
2  
3 Next, a series of aqueous photo-PISA reactions under the same mild polymerization  
4 conditions were carried out for 90 min for the development of PSar<sub>59</sub>-*b*-PHPMA<sub>n</sub> diblock  
5 copolymer nano-objects of different morphologies by targeting various DPs of the core-  
6 forming PHPMA block ( $DP_{\text{PHPMA}} = 100, 200, 300, \text{ and } 400$ ) and total solids concentrations  
7 ( $[\text{solids}] = 10, 15, \text{ and } 20 \text{ wt\%}$ ). In all cases complete monomer conversion ( $\geq 98\%$ ) was  
8 achieved in 90 min of irradiation time, as determined by <sup>1</sup>H-NMR spectroscopic analysis in  
9 methanol-*d*<sub>4</sub> of the crude copolymer samples (Table S1, SI). The PSar<sub>59</sub>-*b*-PHPMA<sub>n</sub> nano-  
10 object samples were purified by consecutive centrifugation-resuspension cycles in DI water  
11 for the removal of unreacted monomer (Figure S4, SI). Based on SEC analysis of lyophilized  
12 samples using 5 mM NH<sub>4</sub>BF<sub>4</sub> in DMF as the eluent, the well-controlled character of photo-  
13 PISA reactions at different solids content was revealed. Specifically, in all cases symmetrical  
14 monomodal molecular weight distributions were observed shifting linearly toward higher  
15 molecular weight ( $M_n$ ) values upon increasing the DP of PHPMA with no apparent trace of  
16 bimolecular termination (Figures 2C and S5, SI). Based on SEC RI chromatograms of PSar<sub>59</sub>-  
17 *b*-PHPMA<sub>n</sub> diblock copolymers, a low molecular weight peak that corresponds to non-  
18 separated and non-functionalized PSar<sub>59</sub> homopolymer (~4–5% of PSar<sub>59</sub>-CEPA macro-CTA  
19 trace in all cases, ca. 2% from <sup>1</sup>H-NMR analysis) is observed, but since it doesn't contribute  
20 to RAFT-mediated chain-extensions of PHPMA or affect the overall nano-object  
21 characteristics it was not taken into consideration for the calculation of  $M_n$  and  $D_M$  values of  
22 the main PSar<sub>59</sub>-*b*-PHPMA<sub>n</sub> diblock copolymer peak in each case (Figure S6, SI).  
23 Importantly, for a series of samples with specified block copolymer composition (i.e. same  
24 target DP of PHPMA) at different total solids concentration ranging from 10-20 wt%,  
25 comparable  $M_n$  values were measured throughout. Low dispersity values were calculated  
26  
27  
28  
29  
30  
31  
32  
33  
34  
35  
36  
37  
38  
39  
40  
41  
42  
43  
44  
45  
46  
47  
48  
49  
50  
51  
52  
53  
54  
55  
56  
57  
58  
59  
60

1  
2  
3 when targeting shorter PHPMA blocks with increasing  $D_M$  upon gradually increasing either  
4 the DP of the core-forming block or the total solids content (Figure 2D and Table S1). This  
5 behavior of  $M_n$  and  $D_M$  values' progression is typical for dispersion PISA systems.  
6  
7

8  
9 Exhaustive dry-state stained transmission electron microscopy (TEM) imaging along with  
10 dynamic light scattering (DLS) and zeta-potential analyses were used for the characterization  
11 of PSar<sub>59</sub>-*b*-PHPMA<sub>n</sub> block copolymer nano-objects in solution (Figures S7-S18 and Table  
12 S2, SI). Morphologies evolving from spherical micelles (S - spheres) to worm-like micelles  
13 (W - worms) and vesicular nanostructures (V - vesicles) along with intermediate mixed  
14 morphologies were observed upon targeting higher DPs of the core-forming PHPMA block  
15 and solids concentration. In particular, a mixture of spheres and short worms was obtained in  
16 the case of PSar<sub>59</sub>-*b*-PHPMA<sub>100</sub> diblock copolymer system at [solids] = 10 and 15 wt%, while  
17 a pure phase of worms could be accessed for the same block copolymer composition at 20  
18 wt%, as sphere-sphere fusion is more favorable at higher solids content. This was evident  
19 macroscopically by the formation of a clear free-standing gel in the reaction vial after photo-  
20 PISA. In all three cases, low hydrodynamic diameter ( $D_h$ ) and polydispersity (PD) values were  
21 measured ranging from 29 - 47 nm and 0.06 - 0.16, respectively, accompanied by narrow  
22 particle size distributions. Aqueous photo-PISA reaction targeting  $DP_{\text{PHPMA}} = 200$  at [solids]  
23 = 10 wt% lead to the formation of a mixed phase of all three morphologies (S+W+V), due to  
24 coexistence of two particle populations initially indicated by DLS analysis and shown by  
25 TEM imaging. A mixture of worm-like micelles and spherical vesicles was formed for the  
26 same DP of PHPMA at [solids] = 15 and 20 wt%. In these cases  $D_h$  and PD values were found  
27 to be relatively higher ( $D_h = 200 - 500$  nm and PD = 0.13 - 0.36) compared to the ones  
28 corresponding to PSar<sub>59</sub>-*b*-PHPMA<sub>100</sub> due to existence of mixed morphologies of small and  
29  
30  
31  
32  
33  
34  
35  
36  
37  
38  
39  
40  
41  
42  
43  
44  
45  
46  
47  
48  
49  
50  
51  
52  
53  
54  
55  
56  
57  
58  
59  
60

1  
2  
3 larger nano-objects. For  $DP_{\text{PHPMA}} = 300$  at  $[\text{solids}] = 10 \text{ wt}\%$ , an intermediate morphology  
4  
5 between worms and vesicles was observed, while pure vesicular morphologies were formed  
6  
7 at higher solids concentrations for the same target DP of PHPMA. Interestingly, a pure phase  
8  
9 of long tubular vesicles was detected for  $\text{PSar}_{59}\text{-}b\text{-PHPMA}_{300}$  at  $[\text{solids}] = 15 \text{ wt}\%$  of average  
10  
11  $D_h = 1360 \text{ nm}$  and  $PD = 0.22$  showing great promise for nanocarrier design applications as it  
12  
13 is proven that non-spherical particles exhibit longer circulation times *in vivo* and could be  
14  
15 more easily uptaken by cells.<sup>64</sup> In the case of 20 wt% total solids content for  $DP_{\text{PHPMA}} = 300$ ,  
16  
17 micron-sized oligolamellar vesicles of relatively low PD were detected by dry-state TEM  
18  
19 imaging. More importantly, pure spherical and elongated unilamellar vesicles with  $D_h = 321$   
20  
21 nm and narrow particles' size distribution were obtained for  $\text{PSar}_{59}\text{-}b\text{-PHPMA}_{400}$  formed at  
22  
23 10 wt% that could potentially be utilized for nanoreactor development. Finally, a mixture of  
24  
25 elongated tubular and multilamellar vesicles was formed in case of  $DP_{\text{PHPMA}} = 400$  at  $[\text{solids}]$   
26  
27 = 15 wt%, while an intriguing morphology of large perforated vesicles with  $D_h = 1515 \text{ nm}$   
28  
29 and  $PD = 0.22$  was observed at 20 wt% solids content. The unusual higher-order vesicular  
30  
31 morphologies observed at exceedingly high DPs and wt% of PHPMA are mainly attributed  
32  
33 to the development of significant hydrophobic interactions between the PHPMA cores and  
34  
35 the short hydrophobic segment of hexylamine located in front of the hydrophilic stabilizer  
36  
37 block of PSar that could promote further entanglement of the polymer chains and formation  
38  
39 of loops potentially aiding the fabrication of flower-like nanostructures.

40  
41  
42 Based on the obtained results, a detailed phase diagram was constructed to summarize the  
43  
44 observed nano-object morphologies of different  $\text{PSar}_{59}\text{-}b\text{-PHPMA}_n$  formulations developed  
45  
46 upon varying  $DP_{\text{PHPMA}}$  and  $[\text{solids}]$  (wt%) and to allow for the facile reproducibility of our  
47  
48 findings (Figure 3). Importantly, in all  $\text{PSar}_{59}\text{-}b\text{-PHPMA}_n$  nano-object formulations, zeta-

potential values of around 0 mV (zeta-potential =  $-0.15 - +0.07$  mV) were measured from microelectrophoretic analysis at neutral pH that were independent of pH variations from acidic (pH = 4.0) to basic (pH = 9.0) values (Table S2, SI), revealing the absence of net charges on the outer surface of particles and their promising “stealth” character as they can prevent the activation of the immune system upon insertion to the body.

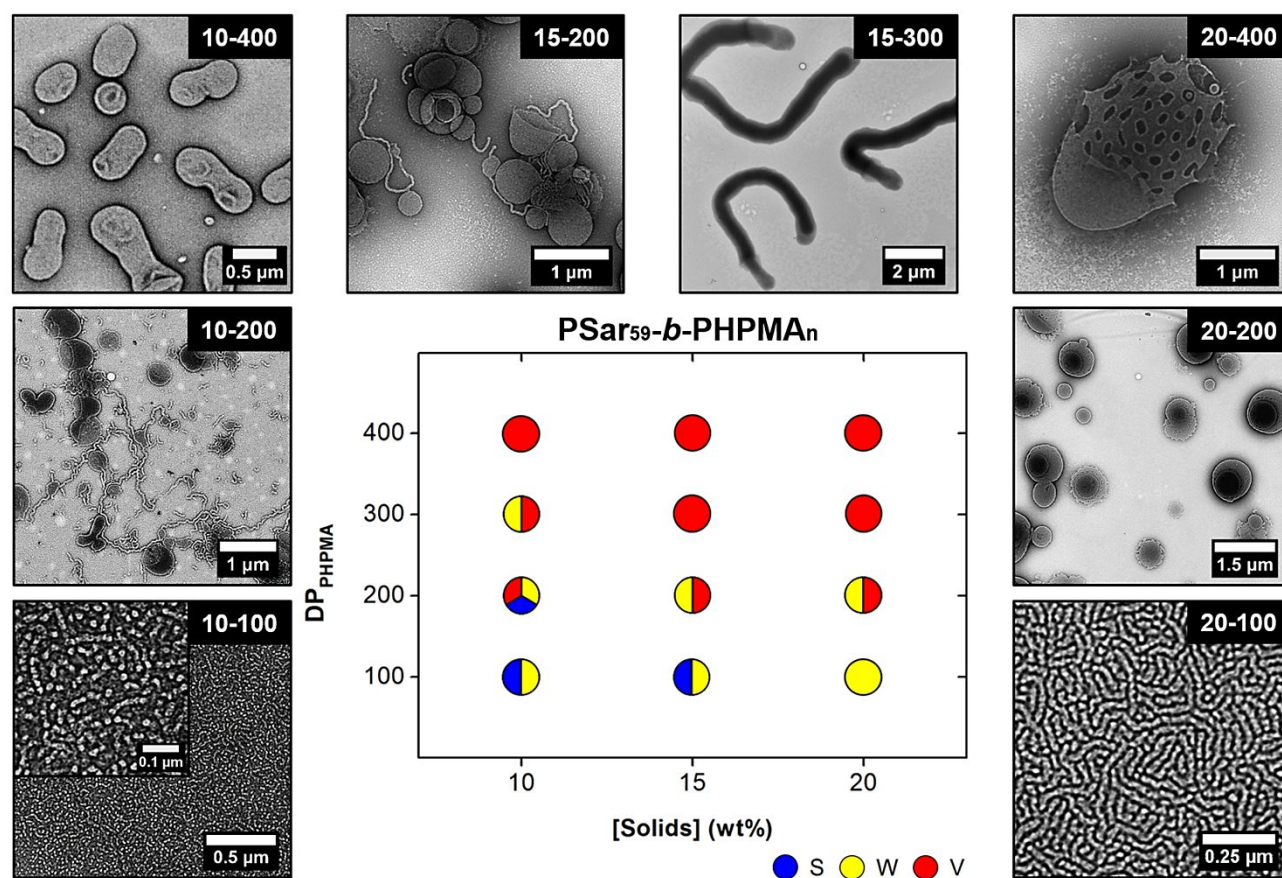


**Figure 3.** Detailed morphologies diagram for  $PSar_{59}-b-PHPMA_n$  diblock copolymer nano-objects prepared *via* aqueous RAFT-mediated photo-PISA of HPMA by varying the total solids content and DP of PHPMA, along with representative dry-state TEM images of different formulations, stained with 1 wt% uranyl acetate (UA) solution. Key: S – spherical micelles (blue), W – worm-like micelles (yellow), V – vesicles (red).



1  
2  
3 **Colloidal stability of PSar<sub>59</sub>-*b*-PHPMA<sub>400</sub> unilamellar vesicles and resistance against**  
4 **degradation by proteolytic enzymes.** Based on the constructed morphologies diagram, the

5  
6 developed PSar<sub>59</sub>-*b*-PHPMA<sub>400</sub> unilamellar vesicles formed at 10 wt% solids as a pure  
7 morphology were isolated and their potential use for nanoreactor fabrication and future *in*  
8 *vitro* and *in vivo* studies was explored. Additionally, the resistance of both empty and enzyme-  
9 loaded vesicles against a series of different proteases was also assessed.

10  
11 First, the colloidal stability of empty PSar<sub>59</sub>-*b*-PHPMA<sub>400</sub> vesicles in a range of complex  
12 media (i.e. DI water, fetal bovine serum (FBS) and cell culture medium) was evaluated, by  
13 monitoring the  $D_h$  changes over time using DLS upon incubation at 37 °C for a total time  
14 period of 72 h (Figure S19, SI). Not surprisingly, the average size of vesicles in DI water  
15 didn't change significantly over extended incubation periods ranging from 340 to 380 nm. In  
16 the case of vesicles incubated in aqueous FBS solution, a negligible  $D_h$  increase to 405 nm  
17 was observed after 24 h of incubation time which was more evident after 72 h ( $D_h = 448$  nm),  
18 indicating slow time-dependent agglomeration of particles with blood components such as  
19 serum proteins (e.g. albumins and globulins).<sup>62</sup> On the contrary, for empty vesicles incubated  
20 in cell growth medium, a minor  $D_h$  decrease was observed after 24 h of incubation time to  
21 220 nm while their size remained constant for the rest of the study. Overall, the obtained  
22 results revealed the good colloidal properties of PSar<sub>59</sub>-*b*-PHPMA<sub>400</sub> vesicles in physiological  
23 media for prolonged time periods.

24  
25 Additionally, to further assess the effect of common proteolytic enzymes on the PSar  
26 poly(peptoid) corona of PSar<sub>59</sub>-*b*-PHPMA<sub>400</sub> vesicles and the potential ability of the formed  
27 nanostructures to act as protective cages of delicate enzymes for development of vesicular  
28 nanoreactors, particle solutions at 10-fold dilution from original concentration were incubated  
29  
30  
31  
32  
33  
34  
35  
36  
37  
38  
39  
40  
41  
42  
43  
44  
45  
46  
47  
48  
49  
50  
51  
52  
53  
54  
55  
56  
57  
58  
59  
60

1  
2  
3 with a series of proteases (i.e.  $\alpha$ -chymotrypsin, trypsin and pepsin) at 37 °C and appropriate  
4 pH for a period of 72 h (Figure 4). Structural and molecular characteristics' changes of empty  
5  
6 PSar<sub>59</sub>-*b*-PHPMA<sub>400</sub> were monitored by DLS and SEC analyses and dry-state TEM imaging  
7  
8 for determination of the ability of hydrophilic and non-ionic PSar<sub>59</sub> stabilizer block to resist  
9  
10 proteolysis. Size variations of the vesicle solutions incubated with either  $\alpha$ -chymotrypsin ( $\alpha$ -  
11  
12 CT) or trypsin at pH = 7.0 and pepsin at pH = 1.8 were measured by DLS analysis (Figure  
13  
14 4A). In case of  $\alpha$ -CT and trypsin, the overall dimensions of particles remained constant in the  
15  
16 range of 305-335 nm for the total incubation period of 72 h, while for pepsin a slight size  
17  
18 increase to 380 nm was monitored after 24 h mainly attributed to the exceedingly low pH  
19  
20 level of the solution affecting the measurements upon extended incubation time periods. Near-  
21  
22 identical SEC molecular weight distributions were recorded for lyophilized samples in all  
23  
24 three cases with  $M_n$  and  $D_M$  values being similar to those of empty PSar<sub>59</sub>-*b*-PHPMA<sub>400</sub>  
25  
26 diblock copolymers formed by aqueous photo-PISA at 10 wt% (Figure 4B), showing no  
27  
28 apparent peptoid bond hydrolysis taking place. Dry-state TEM imaging of empty vesicles  
29  
30 after 72 h of incubation time with each protease proved that no changes in shape and size of  
31  
32 nano-objects occurred showing their excellent stability toward biodegradation from various  
33  
34 proteolytic enzymes (Figures 4C and S20, SI).

35  
36  
37 Based on these findings, the ability of PSar<sub>59</sub>-*b*-PHPMA<sub>400</sub> vesicles to protect other sensitive  
38  
39 hydrophilic enzymes from proteolysis by encapsulation in their inner aqueous lumen compared to  
40  
41 free enzymes was further investigated. Horseradish peroxidase (HRP) was selected as a model  
42  
43 enzyme for encapsulation into PSar<sub>59</sub>-*b*-PHPMA<sub>400</sub> vesicles *via* a one-pot photo-PISA  
44  
45 methodology previously described by our group.<sup>57-59</sup> In these studies, it was shown that such  
46  
47 enzymes could tolerate photo-PISA reaction conditions, retain activity and communicate with the  
48  
49  
50  
51  
52  
53  
54  
55  
56  
57  
58  
59  
60

1  
2  
3 external aqueous environment by passive diffusion of small molecules through the semipermeable  
4 and relatively hydrated PHPMA membrane of vesicles providing a read-out of permeability.  
5  
6 Indeed, control experiments of either purging a HRP solution with N<sub>2</sub> (g) for 15 min or exposure  
7  
8 to 405 nm irradiation for 90 min after N<sub>2</sub> (g) bubbling showed no loss of enzyme activity as  
9  
10 compared to the untreated enzyme (Figure S21, SI). Purified HRP-loaded vesicular nanoreactors  
11  
12 and free HRP were incubated with either a-CT or trypsin at pH = 7.0 for 72 h, and their relative  
13  
14 activities were determined by colorimetric assays at  $\lambda = 492$  nm over time and were normalized  
15  
16 against control experiments of HRP-loaded vesicles and free enzyme incubated solely with  
17  
18 phosphate buffer at pH = 7.0 in absence of proteases. It should be noted that pepsin was not used  
19  
20 for incubation of HRP-loaded vesicles as the optimum pH ranges of the two enzymes differ  
21  
22 significantly. As shown in Figure 4D, quantitative retention of activity was achieved in case of  
23  
24 HRP-loaded vesicles after 18 and 72 h of incubation time with either a-CT (96%) or trypsin (92%).  
25  
26 On the contrary, a significant loss of activity of 29.2% for a-CT and 41% for trypsin was noticed  
27  
28 in case of free HRP attributed to gradual enzyme degradation from the different proteases after 18  
29  
30 h. An additional activity decrease to 54.9% for a-CT and 32.9% for trypsin was measured for the  
31  
32 free enzyme solution after 72 h, clearly showing the robust nature and protective character of PSar-  
33  
34 based vesicles toward other encapsulated biomolecules.  
35  
36  
37  
38  
39  
40  
41

42 Importantly, when performing the described studies to determine the resistance against proteolytic  
43  
44 degradation of purified empty and HRP-loaded PEG<sub>113</sub>-*b*-PHPMA<sub>400</sub> unilamellar vesicles of  
45  
46 similar size and overall characteristics previously developed by our group,<sup>42</sup> a near-identical  
47  
48 retention of enzyme activity was observed in the case of HRP-loaded vesicles after 18 and 72 h of  
49  
50 incubation time with either a-CT or trypsin. However, a significant  $D_h$  and PD increase was  
51  
52 monitored in the case of empty PEG<sub>113</sub>-*b*-PHPMA<sub>400</sub> unilamellar vesicles after 18 h of incubation  
53  
54  
55  
56  
57  
58  
59  
60

time with different proteases (a-CT, trypsin or pepsin), as judged by DLS analysis, mainly attributed to the enhanced protein-induced particle aggregation that occurs in this case after a certain incubation period (Figure S22, SI).

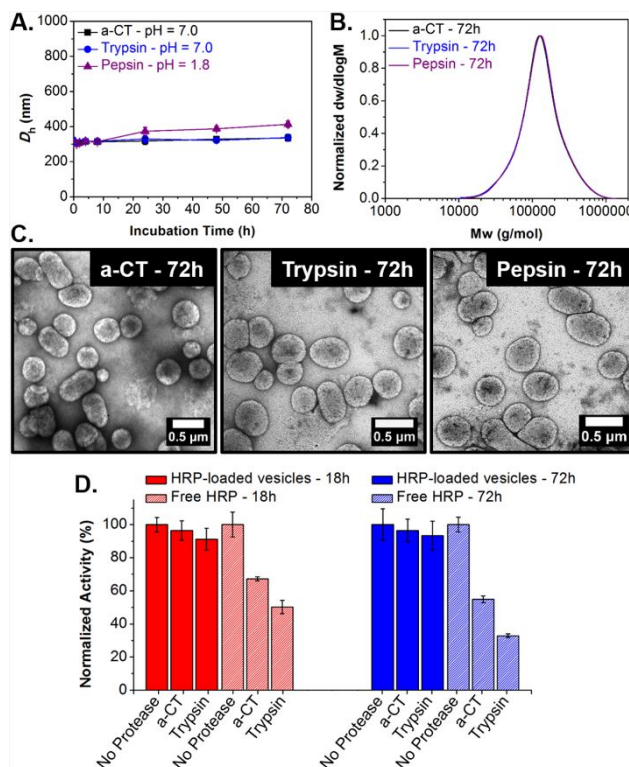


**Figure 4.** (A) Monitoring of hydrodynamic diameter ( $D_h$ ) changes of empty PSAr<sub>59</sub>-b-PHPMA<sub>400</sub> vesicles in 100 mM PB upon incubation with a-CT (pH = 7.0), trypsin (pH = 7.0) or pepsin (pH = 1.8) at 37 °C for 72 h (the error bars show the standard deviation from five repeat measurements). (B) Normalized SEC RI molecular weight distributions for PSAr<sub>59</sub>-b-PHPMA<sub>n</sub> diblock copolymers after incubation with a-CT (pH = 7.0), trypsin (pH = 7.0) or pepsin (pH = 1.8) at 37 °C for 72 h.  $M_n$  and  $D_M$  values were calculated from PMMA standards using 5 mM NH<sub>4</sub>BF<sub>4</sub> in DMF as the eluent. (C) Representative dry-state TEM images of empty PSAr<sub>59</sub>-b-PHPMA<sub>400</sub> vesicles after incubation with a-CT (pH = 7.0), trypsin (pH = 7.0) or pepsin (pH = 1.8) for 72 h, stained with 1 wt% UA. (D) Normalized relative activities of HRP-loaded PSAr<sub>59</sub>-b-PHPMA<sub>400</sub> vesicles and free HRP after incubation with a-CT or trypsin at 37 °C for 18 h (red) and 72 h (blue) (the error shows the standard deviation from four repeat measurements). The normalized relative activities are defined as the ratio between the

1  
2  
3 absorbance of the samples and the absorbance of untreated HRP-loaded vesicles or free HRP,  
4 respectively, at the end point of the enzymatic assay (end point = 30 min,  $\lambda = 492$  nm).  
5  
6  
7  
8  
9

## 10 CONCLUSIONS

11  
12  
13 To conclude, we demonstrate an efficient methodology for the fabrication of poly(peptoid)-  
14 based block copolymer nano-objects with predictable morphologies at high concentrations  
15 by combining living NCA ROP and aqueous RAFT-mediated photo-PISA. In particular,  
16 poly(sarcosine) was utilized as a novel hydrophilic stabilizer block for controlled RAFT  
17 chain-extensions of a methacrylate monomer able to undergo PISA under aqueous  
18 dispersion polymerization conditions targeting different DPs of the core-forming block and  
19 total solids concentrations. A diverse set of nano-object morphologies including higher-  
20 order structures was obtained, as evidenced by the construction of a phase diagram. The  
21 colloidal stability of single phase vesicles and their ability to encapsulate hydrophilic  
22 enzymes protecting them from proteolysis were thoroughly assessed and compared to their  
23 PEG-based counterparts, showing great promise for use of the developed materials in  
24 various biomedical applications. Our findings circumvent the current limitations of  
25 conventional block copolymer self-assembly techniques, such as dilute conditions and  
26 multiple laborious post-polymerization processing and purification steps for targeting  
27 certain morphologies, underlining the potential of poly(sarcosine) as an alternative corona-  
28 forming polymer to PEG-derived polymers for fabrication of PISA nano-objects with bio-  
29 relevant character.  
30  
31  
32  
33  
34  
35  
36  
37  
38  
39  
40  
41  
42  
43  
44  
45  
46  
47  
48  
49  
50  
51  
52  
53  
54  
55  
56  
57  
58  
59  
60

1  
2  
3 ASSOCIATED CONTENT  
4  
5

6 **Supporting Information**  
7

8  
9 The Supporting Information is available free of charge on the ACS Publications website at DOI:  
10  
11 10.1021/acs.bio-mac.xbxxxxx.  
12  
13

14  
15 Materials and characterization methods, additional NMR, FT-IR, SEC and DLS data,  
16  
17 additional dry-state TEM images, HRP control experiments and colloidal stability results.  
18  
19

20 AUTHOR INFORMATION  
21

22  
23 **Corresponding Authors**  
24

25  
26 \*Email: [nikolaos.hadjichristidis@kaust.edu.sa](mailto:nikolaos.hadjichristidis@kaust.edu.sa)  
27

28 \*Email: [r.oreilly@bham.ac.uk](mailto:r.oreilly@bham.ac.uk)  
29  
30

31 **Author Contributions**  
32

33  
34 The manuscript was written through contributions of all authors. All authors have given approval  
35  
36 to the final version of the manuscript.  
37  
38

39 **Notes**  
40

41 The authors declare no competing financial interest.  
42  
43  
44

45 ACKNOWLEDGEMENTS  
46

47  
48 This work was supported by the ERC (grant number 615142), EPSRC and King Abdullah  
49  
50 University of Science and Technology (KAUST).  
51  
52  
53

54 REFERENCES  
55  
56  
57  
58  
59  
60

1. Knop, K.; Hoogenboom, R.; Fischer, D.; Schubert, U. S., Poly(ethylene glycol) in Drug Delivery: Pros and Cons as Well as Potential Alternatives. *Angew. Chem. Int. Ed.* **2010**, *49*, (36), 6288-6308.
2. Jokerst, J. V.; Lobovkina, T.; Zare, R. N.; Gambhir, S. S., Nanoparticle PEGylation for imaging and therapy. *Nanomedicine* **2011**, *6*, (4), 715-728.
3. Cui, S.; Pan, X.; Gebru, H.; Wang, X.; Liu, J.; Liu, J.; Li, Z.; Guo, K., Amphiphilic star-shaped poly(sarcosine)-block-poly( $\epsilon$ -caprolactone) diblock copolymers: one-pot synthesis, characterization, and solution properties. *J. Mater. Chem. B* **2017**, *5*, (4), 679-690.
4. Veronese, F. M.; Pasut, G., PEGylation, successful approach to drug delivery. *Drug Discov. Today* **2005**, *10*, (21), 1451-1458.
5. Turecek, P. L.; Bossard, M. J.; Schoetens, F.; Ivens, I. A., PEGylation of Biopharmaceuticals: A Review of Chemistry and Nonclinical Safety Information of Approved Drugs. *J. Pharm. Sci.* **2016**, *105*, (2), 460-475.
6. Jo, S.; Park, K., Surface modification using silanated poly(ethylene glycol)s. *Biomaterials* **2000**, *21*, (6), 605-616.
7. Fruijtier-Pölloth, C., Safety assessment on polyethylene glycols (PEGs) and their derivatives as used in cosmetic products. *Toxicology* **2005**, *214*, (1), 1-38.
8. Wang, Z.; Song, J.; Zhang, S.; Xu, X.-Q.; Wang, Y., Formulating Polyethylene Glycol as Supramolecular Emulsifiers for One-Step Double Emulsions. *Langmuir* **2017**, *33*, (36), 9160-9169.
9. Lee, Y.-A.; Kim, Y.-H.; Kim, B.-J.; Jung, M.-S.; Auh, J.-H.; Seo, J.-T.; Park, Y.-S.; Lee, S.-H.; Ryu, B.-Y., Cryopreservation of Mouse Spermatogonial Stem Cells in Dimethylsulfoxide and Polyethylene Glycol1. *Biol. Reprod.* **2013**, *89*, (5), 109, 1-9.
10. Harris, J. M.; Chess, R. B., Effect of pegylation on pharmaceuticals. *Nat. Rev. Drug Discovery* **2003**, *2*, 214-221.
11. Ishida, T.; Harada, M.; Wang, X. Y.; Ichihara, M.; Irimura, K.; Kiwada, H., Accelerated blood clearance of PEGylated liposomes following preceding liposome injection: Effects of lipid dose and PEG surface-density and chain length of the first-dose liposomes. *J. Controlled Release* **2005**, *105*, (3), 305-317.
12. Garay, R. P.; El-Gewely, R.; Armstrong, J. K.; Garratty, G.; Richette, P., Antibodies against polyethylene glycol in healthy subjects and in patients treated with PEG-conjugated agents. *Expert Opin. Drug Deliv.* **2012**, *9*, (11), 1319-1323.
13. Deng, Y.; Zou, T.; Tao, X.; Semetey, V.; Trepout, S.; Marco, S.; Ling, J.; Li, M.-H., Poly( $\epsilon$ -caprolactone)-block-polysarcosine by Ring-Opening Polymerization of Sarcosine N-Thiocarboxyanhydride: Synthesis and Thermoresponsive Self-Assembly. *Biomacromolecules* **2015**, *16*, (10), 3265-3274.
14. Hu, Y.; Hou, Y.; Wang, H.; Lu, H., Polysarcosine as an Alternative to PEG for Therapeutic Protein Conjugation. *Bioconjugate Chem.* **2018**, *29*, (7), 2232-2238.
15. Pelegri-O'Day, E. M.; Lin, E.-W.; Maynard, H. D., Therapeutic Protein-Polymer Conjugates: Advancing Beyond PEGylation. *J. Am. Chem. Soc.* **2014**, *136*, (41), 14323-14332.
16. Zhang, H.; Grinstaff, M. W., Recent Advances in Glycerol Polymers: Chemistry and Biomedical Applications. *Macromol. Rapid Commun.* **2014**, *35*, (22), 1906-1924.
17. Hoogenboom, R., Poly(2-oxazoline)s: A Polymer Class with Numerous Potential Applications. *Angew. Chem. Int. Ed.* **2009**, *48*, (43), 7978-7994.
18. Liarou, E.; Varlas, S.; Skoulas, D.; Tsimblouli, C.; Sereti, E.; Dimas, K.; Iatrou, H., Smart polymersomes and hydrogels from polypeptide-based polymer systems through  $\alpha$ -amino acid N-

1  
2  
3 carboxyanhydride ring-opening polymerization. From chemistry to biomedical applications. *Prog.*  
4 *Polym. Sci.* **2018**, 83, 28-78.

5  
6 19. Secker, C.; Brosnan, S. M.; Luxenhofer, R.; Schlaad, H., Poly( $\alpha$ -Peptoids) Revisited:  
7 Synthesis, Properties, and Use as Biomaterial. *Macromol. Biosci.* **2015**, 15, (7), 881-891.

8  
9 20. Gangloff, N.; Ulbricht, J.; Lorson, T.; Schlaad, H.; Luxenhofer, R., Peptoids and  
10 Polypeptoids at the Frontier of Supra- and Macromolecular Engineering. *Chem. Rev.* **2016**, 116,  
11 (4), 1753-1802.

12  
13 21. Mudd, S. H.; Ebert, M. H.; Scriver, C. R., Labile methyl group balances in the human: The  
14 role of sarcosine. *Metabolism* **1980**, 29, (8), 707-720.

15  
16 22. Weber, B.; Seidl, C.; Schwiertz, D.; Scherer, M.; Bleher, S.; Süß, R.; Barz, M.,  
17 Polysarcosine-Based Lipids: From Lipopolypeptoid Micelles to Stealth-Like Lipids in Langmuir  
18 Blodgett Monolayers. *Polymers* **2016**, 8, (12), 427.

19  
20 23. Birke, A.; Ling, J.; Barz, M., Polysarcosine-containing copolymers: Synthesis,  
21 characterization, self-assembly, and applications. *Prog. Polym. Sci.* **2018**, 81, 163-208.

22  
23 24. Fokina, A.; Klinker, K.; Braun, L.; Jeong, B. G.; Bae, W. K.; Barz, M.; Zentel, R.,  
24 Multidentate Polysarcosine-Based Ligands for Water-Soluble Quantum Dots. *Macromolecules*  
25 **2016**, 49, (10), 3663-3671.

26  
27 25. Hadjichristidis, N.; Iatrou, H.; Pitsikalis, M.; Sakellariou, G., Synthesis of Well-Defined  
28 Polypeptide-Based Materials via the Ring-Opening Polymerization of  $\alpha$ -Amino Acid N-  
29 Carboxyanhydrides. *Chem. Rev.* **2009**, 109, (11), 5528-5578.

30  
31 26. Zhang, D.; Lahasky, S. H.; Guo, L.; Lee, C.-U.; Lavan, M., Polypeptoid Materials: Current  
32 Status and Future Perspectives. *Macromolecules* **2012**, 45, (15), 5833-5841.

33  
34 27. Birke, A.; Huesmann, D.; Kelsch, A.; Weilbacher, M.; Xie, J.; Bros, M.; Bopp, T.; Becker,  
35 C.; Landfester, K.; Barz, M., Polypeptoid-block-polypeptide Copolymers: Synthesis,  
36 Characterization, and Application of Amphiphilic Block Copolypept(o)ides in Drug Formulations  
37 and Miniemulsion Techniques. *Biomacromolecules* **2014**, 15, (2), 548-557.

38  
39 28. Huesmann, D.; Sevenich, A.; Weber, B.; Barz, M., A head-to-head comparison of  
40 poly(sarcosine) and poly(ethylene glycol) in peptidic, amphiphilic block copolymers. *Polymer*  
41 **2015**, 67, 240-248.

42  
43 29. Fetsch, C.; Gaitzsch, J.; Messenger, L.; Battaglia, G.; Luxenhofer, R., Self-Assembly of  
44 Amphiphilic Block Copolypeptoids – Micelles, Worms and Polymersomes. *Sci. Rep.* **2016**, 6,  
45 33491.

46  
47 30. Weber, B.; Kappel, C.; Scherer, M.; Helm, M.; Bros, M.; Grabbe, S.; Barz, M., PeptoSomes  
48 for Vaccination: Combining Antigen and Adjuvant in Polypept(o)ide-Based Polymersomes.  
49 *Macromol. Biosci.* **2017**, 17, (10), 1700061.

50  
51 31. Makino, A.; Hara, E.; Hara, I.; Ozeki, E.; Kimura, S., Size Control of Core-Shell-type  
52 Polymeric Micelle with a Nanometer Precision. *Langmuir* **2014**, 30, (2), 669-674.

53  
54 32. Kim, C. J.; Ueda, M.; Imai, T.; Sugiyama, J.; Kimura, S., Tuning the Viscoelasticity of  
55 Peptide Vesicles by Adjusting Hydrophobic Helical Blocks Comprising Amphiphilic  
56 Polypeptides. *Langmuir* **2017**, 33, (22), 5423-5429.

57  
58 33. Warren, N. J.; Mykhaylyk, O. O.; Mahmood, D.; Ryan, A. J.; Armes, S. P., RAFT aqueous  
59 dispersion polymerization yields poly(ethylene glycol)-based diblock copolymer nano-objects  
60 with predictable single phase morphologies. *J. Am. Chem. Soc.* **2014**, 136, (3), 1023-33.

61  
62 34. Warren, N. J.; Armes, S. P., Polymerization-induced self-assembly of block copolymer  
63 nano-objects via RAFT aqueous dispersion polymerization. *J. Am. Chem. Soc.* **2014**, 136, (29),  
64 10174-85.



- 1  
2  
3 35. Canning, S. L.; Smith, G. N.; Armes, S. P., A Critical Appraisal of RAFT-Mediated  
4 Polymerization-Induced Self-Assembly. *Macromolecules* **2016**, 49, (6), 1985-2001.
- 5 36. Derry, M. J.; Fielding, L. A.; Armes, S. P., Polymerization-induced self-assembly of block  
6 copolymer nanoparticles via RAFT non-aqueous dispersion polymerization. *Prog. Polym. Sci.*  
7 **2016**, 52, 1-18.
- 8 37. Wang, G.; Schmitt, M.; Wang, Z.; Lee, B.; Pan, X.; Fu, L.; Yan, J.; Li, S.; Xie, G.;  
9 Bockstaller, M. R.; Matyjaszewski, K., Polymerization-Induced Self-Assembly (PISA) Using  
10 ICAR ATRP at Low Catalyst Concentration. *Macromolecules* **2016**, 49, (22), 8605-8615.
- 11 38. Obeng, M.; Milani, A. H.; Musa, M. S.; Cui, Z.; Fielding, L. A.; Farrand, L.; Goulding,  
12 M.; Saunders, B. R., Self-assembly of poly(lauryl methacrylate)-b-poly(benzyl methacrylate)  
13 nano-objects synthesised by ATRP and their temperature-responsive dispersion properties. *Soft*  
14 *Matter* **2017**, 13, (11), 2228-2238.
- 15 39. Qiao, X. G.; Lansalot, M.; Bourgeat-Lami, E.; Charleux, B., Nitroxide-Mediated  
16 Polymerization-Induced Self-Assembly of Poly(poly(ethylene oxide) methyl ether methacrylate-  
17 co-styrene)-b-poly(n-butyl methacrylate-co-styrene) Amphiphilic Block Copolymers.  
18 *Macromolecules* **2013**, 46, (11), 4285-4295.
- 19 40. Qiao, X. G.; Dugas, P. Y.; Charleux, B.; Lansalot, M.; Bourgeat-Lami, E., Nitroxide-  
20 mediated polymerization-induced self-assembly of amphiphilic block copolymers with a  
21 pH/temperature dual sensitive stabilizer block. *Polym. Chem.* **2017**, 8, (27), 4014-4029.
- 22 41. Williams, M.; Penfold, N. J. W.; Lovett, J. R.; Warren, N. J.; Douglas, C. W. I.;  
23 Doroshenko, N.; Verstraete, P.; Smets, J.; Armes, S. P., Bespoke cationic nano-objects via RAFT  
24 aqueous dispersion polymerisation. *Polym. Chem.* **2016**, 7, (23), 3864-3873.
- 25 42. Blackman, L. D.; Doncom, K. E. B.; Gibson, M. I.; O'Reilly, R. K., Comparison of photo-  
26 and thermally initiated polymerization-induced self-assembly: a lack of end group fidelity drives  
27 the formation of higher order morphologies. *Polym. Chem.* **2017**, 8, (18), 2860-2871.
- 28 43. Deng, R.; Derry, M. J.; Mable, C. J.; Ning, Y.; Armes, S. P., Using Dynamic Covalent  
29 Chemistry To Drive Morphological Transitions: Controlled Release of Encapsulated  
30 Nanoparticles from Block Copolymer Vesicles. *J. Am. Chem. Soc.* **2017**, 139, (22), 7616-7623.
- 31 44. Khor, S. Y.; Truong, N. P.; Quinn, J. F.; Whittaker, M. R.; Davis, T. P., Polymerization-  
32 Induced Self-Assembly: The Effect of End Group and Initiator Concentration on Morphology of  
33 Nanoparticles Prepared via RAFT Aqueous Emulsion Polymerization. *ACS Macro Lett.* **2017**, 6,  
34 (9), 1013-1019.
- 35 45. Wright, D. B.; Touve, M. A.; Thompson, M. P.; Gianneschi, N. C., Aqueous-Phase Ring-  
36 Opening Metathesis Polymerization-Induced Self-Assembly. *ACS Macro Lett.* **2018**, 7, (4), 401-  
37 405.
- 38 46. Foster, J. C.; Varlas, S.; Blackman, L. D.; Arkinstall, L. A.; O'Reilly, R. K., Ring-Opening  
39 Metathesis Polymerization in Aqueous Media Using a Macroinitiator Approach. *Angew. Chem.*  
40 *Int. Ed.* **2018**, 57, (33), 10672-10676.
- 41 47. Wright, D. B.; Touve, M. A.; Adamiak, L.; Gianneschi, N. C., ROMPISA: Ring-Opening  
42 Metathesis Polymerization-Induced Self-Assembly. *ACS Macro Lett.* **2017**, 6, (9), 925-929.
- 43 48. Tan, J.; Sun, H.; Yu, M.; Sumerlin, B. S.; Zhang, L., Photo-PISA: Shedding Light on  
44 Polymerization-Induced Self-Assembly. *ACS Macro Lett.* **2015**, 4, (11), 1249-1253.
- 45 49. Yeow, J.; Xu, J.; Boyer, C., Polymerization-Induced Self-Assembly Using Visible Light  
46 Mediated Photoinduced Electron Transfer-Reversible Addition-Fragmentation Chain Transfer  
47 Polymerization. *ACS Macro Lett.* **2015**, 4, (9), 984-990.
- 48  
49  
50  
51  
52  
53  
54  
55  
56  
57  
58  
59  
60

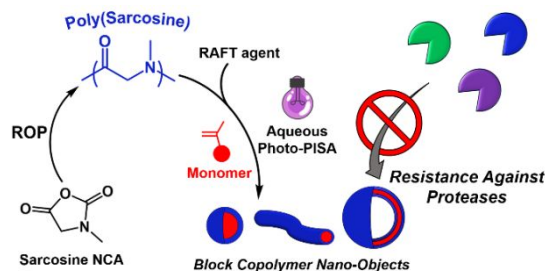
- 1  
2  
3 50. Tan, J.; Bai, Y.; Zhang, X.; Zhang, L., Room temperature synthesis of poly(poly(ethylene  
4 glycol) methyl ether methacrylate)-based diblock copolymer nano-objects via Photoinitiated  
5 Polymerization-Induced Self-Assembly (Photo-PISA). *Polym. Chem.* **2016**, *7*, (13), 2372-2380.
- 6 51. Ng, G.; Yeow, J.; Xu, J.; Boyer, C., Application of oxygen tolerant PET-RAFT to  
7 polymerization-induced self-assembly. *Polym. Chem.* **2017**, *8*, (18), 2841-2851.
- 8 52. Tan, J.; Liu, D.; Bai, Y.; Huang, C.; Li, X.; He, J.; Xu, Q.; Zhang, X.; Zhang, L., An insight  
9 into aqueous photoinitiated polymerization-induced self-assembly (photo-PISA) for the  
10 preparation of diblock copolymer nano-objects. *Polym. Chem.* **2017**, *8*, (8), 1315-1327.
- 11 53. Yeow, J.; Boyer, C., Photoinitiated Polymerization-Induced Self-Assembly (Photo-PISA):  
12 New Insights and Opportunities. *Adv. Sci.* **2017**, *4*, (7), 1700137.
- 13 54. Burrige, K. M.; Wright, T. A.; Page, R. C.; Konkolewicz, D., Photochemistry for Well-  
14 Defined Polymers in Aqueous Media: From Fundamentals to Polymer Nanoparticles to  
15 Bioconjugates. *Macromol. Rapid Commun.* **2018**, *39*, (12), 1800093.
- 16 55. Tan, J.; Zhang, X.; Liu, D.; Bai, Y.; Huang, C.; Li, X.; Zhang, L., Facile Preparation of  
17 CO<sub>2</sub>-Responsive Polymer Nano-Objects via Aqueous Photoinitiated Polymerization-Induced  
18 Self-Assembly (Photo-PISA). *Macromol. Rapid Commun.* **2016**, *38*, (13), 1600508.
- 19 56. Tan, J.; Liu, D.; Bai, Y.; Huang, C.; Li, X.; He, J.; Xu, Q.; Zhang, L., Enzyme-Assisted  
20 Photoinitiated Polymerization-Induced Self-Assembly: An Oxygen-Tolerant Method for  
21 Preparing Block Copolymer Nano-Objects in Open Vessels and Multiwell Plates. *Macromolecules*  
22 **2017**, *50*, (15), 5798-5806.
- 23 57. Blackman, L. D.; Varlas, S.; Arno, M. C.; Fayter, A.; Gibson, M. I.; O'Reilly, R. K.,  
24 Permeable Protein-Loaded Polymersome Cascade Nanoreactors by Polymerization-Induced Self-  
25 Assembly. *ACS Macro Lett.* **2017**, *6*, (11), 1263-1267.
- 26 58. Blackman, L. D.; Varlas, S.; Arno, M. C.; Houston, Z. H.; Fletcher, N. L.; Thurecht, K. J.;  
27 Hasan, M.; Gibson, M. I.; O'Reilly, R. K., Confinement of Therapeutic Enzymes in Selectively  
28 Permeable Polymer Vesicles by Polymerization-Induced Self-Assembly (PISA) Reduces  
29 Antibody Binding and Proteolytic Susceptibility. *ACS Cent. Sci.* **2018**, *4*, (6), 718-723.
- 30 59. Varlas, S.; Blackman, L. D.; Findlay, H. E.; Reading, E.; Booth, P. J.; Gibson, M. I.;  
31 O'Reilly, R. K., Photoinitiated Polymerization-Induced Self-Assembly in the Presence of  
32 Surfactants Enables Membrane Protein Incorporation into Vesicles. *Macromolecules* **2018**, *51*,  
33 (6), 6190-6201.
- 34 60. Weber, B.; Birke, A.; Fischer, K.; Schmidt, M.; Barz, M., Solution Properties of  
35 Polysarcosine: From Absolute and Relative Molar Mass Determinations to Complement  
36 Activation. *Macromolecules* **2018**, *51*, (7), 2653-2661.
- 37 61. Johnson, R. N.; Burke, R. S.; Convertine, A. J.; Hoffman, A. S.; Stayton, P. S.; Pun, S. H.,  
38 Synthesis of Statistical Copolymers Containing Multiple Functional Peptides for Nucleic Acid  
39 Delivery. *Biomacromolecules* **2010**, *11*, (11), 3007-3013.
- 40 62. Bilalis, P.; Tziveleka, L.-A.; Varlas, S.; Iatrou, H., pH-Sensitive nanogates based on poly(l-  
41 histidine) for controlled drug release from mesoporous silica nanoparticles. *Polym. Chem.* **2016**,  
42 *7*, (7), 1475-1485.
- 43 63. Tan, J.; He, J.; Li, X.; Xu, Q.; Huang, C.; Liu, D.; Zhang, L., Rapid synthesis of well-  
44 defined all-acrylic diblock copolymer nano-objects via alcoholic photoinitiated polymerization-  
45 induced self-assembly (photo-PISA). *Polym. Chem.* **2017**, *8*, (44), 6853-6864.
- 46 64. Robertson, J. D.; Yealland, G.; Avila-Olias, M.; Chierico, L.; Bandmann, O.; Renshaw, S.  
47 A.; Battaglia, G., pH-Sensitive Tubular Polymersomes: Formation and Applications in Cellular  
48 Delivery. *ACS Nano* **2014**, *8*, (5), 4650-4661.
- 49  
50  
51  
52  
53  
54  
55  
56  
57  
58  
59  
60

1  
2  
3  
4  
5  
6  
7  
8  
9  
10  
11  
12  
13  
14  
15  
16  
17  
18  
19  
20  
21  
22  
23  
24  
25  
26  
27  
28  
29  
30  
31  
32  
33  
34  
35  
36  
37  
38  
39  
40  
41  
42  
43  
44  
45  
46  
47  
48  
49  
50  
51  
52  
53  
54  
55  
56  
57  
58  
59  
60

## TABLE OF CONTENTS GRAPHIC (TOC)

“Poly(sarcosine)-Based Nano-Objects with Multi-Protease Resistance by Aqueous Photoinitiated Polymerization-Induced Self-Assembly (Photo-PISA)”

*Spyridon Varlas,<sup>a</sup> Panagiotis G. Georgiou,<sup>a,b</sup> Panayiotis Bilalis,<sup>c</sup> Joseph R. Jones,<sup>a</sup> Nikos Hadjichristidis,<sup>c\*</sup> and Rachel K. O'Reilly<sup>a\*</sup>*



Poly(sarcosine)-based diblock copolymer nano-objects with various morphologies were prepared by combining *N*-carboxyanhydride ring-opening polymerization (ROP) and RAFT-mediated photoinitiated polymerization-induced self-assembly (photo-PISA) of a commercially available monomer (2-hydroxypropyl methacrylate), using a poly(sarcosine) macromolecular chain transfer agent. Based on a constructed phase diagram, vesicles were chosen and the resistance of both empty and horseradish peroxidase-loaded ones against degradation by a series of proteolytic enzymes was evaluated.